Gene Therapy (2008), 1–11

www.nature.com/gt

ORIGINAL ARTICLE

# Inhibition of tumor cell growth in the liver by RNA interference-mediated suppression of HIF-1α expression in tumor cells and hepatocytes

Y Takahashi, M Nishikawa and Y Takakura
*Department of Biopharmaceutics and Drug Metabolism, Graduate School of Pharmaceutical Sciences, Kyoto University, Kyoto, Japan*

*Hypoxia-inducible factor-1 (HIF-1) is a ubiquitously expressed oxygen-regulated transcription factor composed of α and β subunits. HIF-1 activates transcription of various genes including those involved in metastatic tumor growth. In the present study, HIF-1α expression in tumor-bearing mouse liver was examined after inoculation of tumor cells into portal vein. We found that tumor-bearing liver showed greatly increased HIF-1α expression. Plasmid DNA (pDNA) expressing short hairpin RNA targeting HIF-1α (pshHIF-1α) was effective in suppressing protein expression of HIF-1α in vitro. Intravenous injection of pshHIF-1α by hydrodynamics-based procedure reduced the HIF-1α protein expression in both normal and tumor cells and tumor cell number in the liver. Pre-injection of pshHIF-1α to mice, by which pDNA was delivered only to liver cells, not to tumor cells, was also effective in reducing the number of tumor cells inoculated 3 days after pDNA injection. These findings indicate that HIF-1α expression is increased in normal liver cells as well as tumor cells, and HIF-1α expression plays an important role in tumor progression. Use of the RNA interference (RNAi) of HIF-1 is an effective strategy for inhibiting tumor cell growth, and both tumor and normal cells can be the target for RNAi-based anticancer treatment.*
Gene Therapy advance online publication, 14 February 2008; doi:10.1038/sj.gt.3303103

**Keywords:** *RNAi; HIF-1α; gene delivery; hydrodynamics-based procedure; hepatic metastasis*

## Introduction

Metastasis, which is the transfer of cancer cells from one organ to other organs, is the most distinctive feature of malignant tumors and is the cause of approximately 90% of human cancer deaths.[1,2] Tumor metastasis is an exceedingly complex process, which occurs through a series of sequential steps that include dissociation from the primary tumor, invasion of adjacent tissues, intravasation, transport through the circulatory system, arrest in small vessels, adhesion to endothelial cells, extravasation and growth in secondary organs.[3] It can be hypothesized that components of the secondary organ, such as endothelial cells, stromal cells, fibroblasts and parenchymal cells, are functionally organized to promote survival and proliferation of metastasizing cancer cells and generate a favorable microenvironment for cancer cells in metastatic sites.[4,5]

Hypoxia initiates a variety of cellular responses including the activation of hypoxia-inducible factor-1 (HIF-1).[6,7] HIF-1 is a ubiquitously expressed heterodimeric transcription factor composed of a constitutively expressed β subunit and an oxygen-regulated α subunit. Under normal oxygen tension, the α subunit is continuously hydroxylated at conserved prolyl and asparaginyl residues and is targeted for degradation by the von Hippel–Lindau ubiquitin E3 ligase complex.[8] In hypoxia, inhibition of hydroxylation results in the stabilization of HIF-1α and its subsequent nuclear entry, which leads to transcriptional activation of target genes that stimulates angiogenesis, such as vascular endothelial growth factor (VEGF), that controls invasion of cancer cells, such as matrix metalloproteinases (MMPs), and promotes metabolic adaptation to hypoxia.[9] In general, tumor cells grow faster than the rate of angiogenesis so that tumor tissues are characterized by internal hypoxia. Therefore, activation of HIF-1 has been described in a variety of human cancers and their metastases.[10,11] Moreover, although the role of HIF-1α in tumor cell growth has not been fully elucidated, our results and those from other groups have demonstrated that HIF-1α expression in tumor tissues is likely to help tumor cell survival and growth.[12,13]

RNA interference (RNAi) is an evolutionary conserved sequence-specific gene silencing mechanism, which can be triggered by small 21- to 25-nt double-stranded small interfering RNA (siRNA) or short hairpin RNA (shRNA) that is processed in the cell to form siRNA.[14,15] Intravascular injection of a large-volume isotonic solution at a high speed is a very efficient method for delivering any solutes, including siRNA- and shRNA-expressing plasmid DNA (pDNA), to liver cells. This procedure, the so-called hydrodynamics-based procedure, has been applied to suppress expression of target genes in the liver.[16,17] In addition to such application, we found that the hydrodynamic

Correspondence: Professor Y Takakura, Department of Biopharmaceutics and Drug Metabolism, Graduate School of Pharmaceutical Sciences, Kyoto University, Sakyo-ku, Kyoto 606-8501, Japan.
E-mail: takakura@pharm.kyoto-u.ac.jp
Received 2 August 2007; revised 4 December 2007; accepted 5 December 2007

administration is also applicable to deliver siRNA- and shRNA-expressing pDNA to tumor cells in the liver.[18] Therefore, the hydrodynamics-based procedure can be an effective method to suppress the growth of tumor cells that are metastasized to the liver. Because the hydrodynamic administration can induce RNAi in both tumor cells in the liver and normal liver cells, suppressing the increased expression of a gene that aggravates the metastatic tumor growth in both tumor and liver cells can be an effective approach in treating hepatic metastasis. To this end, we selected HIF-1α as such a target gene in the present study. We applied the hydrodynamic injection method to administer shRNA-expressing pDNA targeting HIF-1α (pshHIF-1α) and found that the suppression of HIF-1α expression in the liver can suppress the growth of metastasizing tumor cells in that organ. Moreover, selective suppression of HIF-1α expression only in normal liver cells was found to be also effective in inhibiting metastatic tumor growth, indicating that HIF-1α expression in normal cells assisted the tumor progression.

## Results

### *Reduction in protein expression of HIF-1α by shRNA-expressing pDNA*

As previously reported by several groups, an enzyme-linked immunosorbent assay (ELISA) analysis showed that addition of $CoCl_2$ increased the amount of HIF-1α proteins in Colon26 and B16-BL6 cells (Figure 1a). Similar results were obtained when HIF-1α protein levels in Colon26 cells were evaluated by western blot analysis (Figure 1b). Transfection of pshHIF-1α reduced the amount of HIF-1α protein, whereas transfection of control pDNA or pshGFP (green fluorescent protein) hardly affected the level of HIF-1α expression.

Using immunofluorescent staining with HIF-1α-specific antibody, localization of HIF-1α protein in the cells was visualized. While a weak signal of HIF-1α was observed in cytoplasm when cells were incubated without $CoCl_2$, incubation of Colon26 cells with $CoCl_2$ resulted in nuclear accumulation of HIF-1α, which was detected as yellow signals as a result of overlap between the green fluorescence derived from HIF-1α and the red fluorescence derived from nuclear staining (Figure 1c). Transfection of pshHIF-1α reduced the number of cells that show HIF-1α accumulation in their nucleus.

### *Inhibition of HIF-1 transcriptional activity by pshHIF-1α*

To investigate whether pshHIF-1α is effective in suppressing the transcription activity of HIF-1, cells were transfected with a pDNA encoding luciferase gene under the control of hypoxia response element (HRE). In Colon26 cells, HRE-dependent luciferase expression from the reporter pDNA co-transfected with control pDNA or pshGFP was moderately increased by the addition of $CoCl_2$. However, in B16-BL6 cells, HRE-dependent luciferase expression was increased by the addition of $CoCl_2$ compared with Colon26 cells (Figures 2a and b). HRE-dependent luciferase expression in the presence of $CoCl_2$ was almost completely inhibited to about the expression level observed in the absence of $CoCl_2$ by transfection of pshHIF-1α.

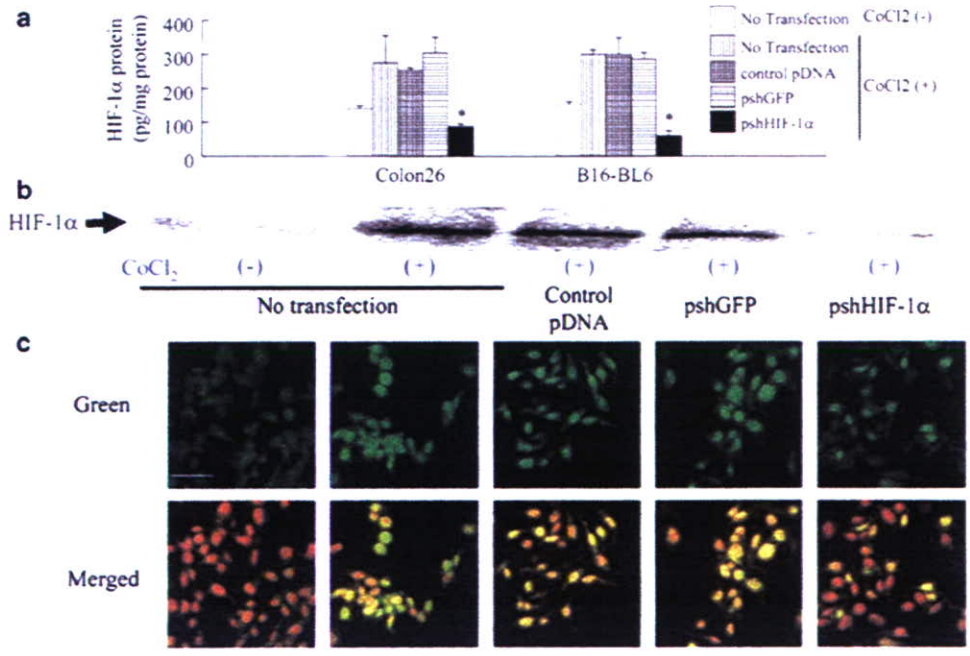


**Figure 1** Hypoxia-inducible factor-1α (HIF-1α) protein expression level in tumor cells following transfection of short hairpin (shRNA)-expressing plasmid DNA (pDNA). Cells were transfected with control pDNA, pshGFP (green fluorescent protein) or pDNA expressing shRNA targeting HIF-1α (pshHIF-1α). At 4 h after transfection, cells were washed with phosphate-buffered saline (PBS) and then cultured with growth medium supplemented with or without 100 μM $CoCl_2$ for an additional 20 h. (**a**) Enzyme-linked immunosorbent assay (ELISA) analysis of HIF-1α protein from cell lysates of Colon26 or B16-BL6 cells. The results are expressed as the mean ± s.d. of three samples. $^*P < 0.05$ for Student's *t*-test versus the control group. (**b**) Western blotting analysis of HIF-1α for cell lysates of Colon26 cells. (**c**) Immunofluorescent staining of HIF-1α in transfected Colon26 cells. HIF-1α protein expression was detected as a green color, and the cell nucleus was stained with propidium iodide (red). Yellow signals indicate that HIF-1α localizes in the cell nucleus. Scale bar = 50 μm.

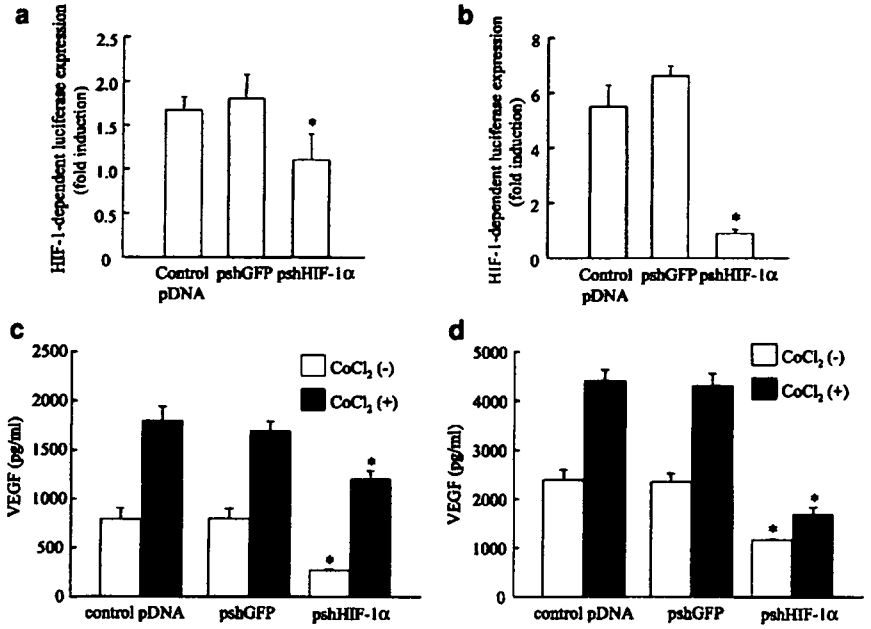


**Figure 2** Suppression of hypoxia-inducible factor-1 (HIF-1)-dependent gene expression by transfection of plasmid DNA (pDNA) expressing shRNA targeting HIF-1α (pshHIF-1α). (**a**, **b**) Suppression of HIF-1-dependent reporter gene expression by pshHIF-1α. pLuc-HRE and phRL-TK were co-transfected with control pDNA, pshGFP (green fluorescent protein) or pshHIF-1α to Colon26 (**a**) or B16-BL6 (**b**) cells. At 4 h after transfection, cells were washed with phosphate-buffered saline (PBS) and cultured in medium with or without 100 μM $CoCl_2$ for an additional 20 h. Luciferase activities were measured 24 h after transfection. The results are expressed as the mean ± s.d. of three samples. (**c**, **d**) Reduction in HIF-1-dependent vascular endothelial growth factor (VEGF) production by pshHIF-1α. Colon26 (**c**) or B16-BL6 (**d**) cells were transfected with control pDNA, pshGFP or pshHIF-1α. At 4 h after transfection, cells were washed with PBS and cultured in medium with or without 100 μM $CoCl_2$ for an additional 44 h. The amount of VEGF protein in the cultured medium was measured 48 h after transfection using enzyme-linked immunosorbent assay (ELISA). The results are expressed as the mean ± s.d. of three samples. $^*P<0.05$ for Student's *t*-test versus the control group.

To further estimate the effect of pshHIF-1α transfection on the expression of VEGF, an endogenous gene product of HIF-1 transcription activity, culture media of tumor cells were collected 48 h after the transfection. The VEGF concentration in the supernatant was measured by ELISA (Figures 2c and d). In both cell lines, about a two-fold increase was detected in the VEGF from $CoCl_2$-treated cells compared with that from untreated cells. In Colon26 cells, transfection of pshHIF-1α reduced VEGF secretion to about one-third or two-thirds of the control values without or with $CoCl_2$, respectively. In B16-BL6 cells, transfection of pshHIF-1α reduced VEGF secretion to about half or one-third of the control values without or with $CoCl_2$, respectively.

### *Increase in HIF-1α expression in the liver by tumor inoculation via the portal vein*

Mice were inoculated with tumor cells into the portal vein, and received an intravenous injection of each pDNA 5 days after tumor inoculation. Then, immunofluorescent staining of liver sections was performed to detect HIF-1α protein expression 7 days after tumor inoculation. Representative images are shown in Figures 3a–g. No significant signal of HIF-1α was observed in the liver sections of naïve mice, sham-operated mice and those receiving control pDNA (Figures 3a–c). In contrast, a strong HIF-1α signal was observed in the liver sections of tumor-bearing mice (Figure 3d). In these pictures, increased HIF-1α expression was mainly observed in hepatic cells. Administration of control pDNA or pshGFP had little effect on HIF-1α expression induced by the inoculation of tumor cells (Figures 3e and f). Moreover, hydrodynamic administration of pshHIF-1α reduced the signal intensity derived from HIF-1α protein compared with other tumor-bearing groups (Figure 3g). By quantitatively analyzing relative areas of the HIF-1α expression (green signal) to the total area in the images, the percentage inhibition by pshHIF-1α was calculated to be about 20–30% of the other tumor-bearing groups. In addition, the administration of pshHIF-1α significantly ($P<0.05$) reduced the mRNA expression of HIF-1α in tumor-bearing liver, from 0.0059 ± 0.0011 copies relative to GAPDH mRNA (the control pDNA-treated group) to 0.0021 ± 0.0005.

### *Suppression of HIF-1α expression in liver by the pre-administration of pshHIF-1α*

As it had been demonstrated that tumor inoculation via the portal vein induced HIF-1α accumulation in liver cells, we investigated whether the delivery of pshHIF-1α only to liver cells, not to tumor cells, affects tumor growth in the liver. To this end, tumor cells were inoculated 3 days after the hydrodynamic administration of pDNAs. Immunofluorescent staining for HIF-1α was performed at 2 days after tumor inoculation to investigate the HIF-1α expression level at that time (Figures 3h–l). Similar to the results of the sample prepared at 7 days after tumor inoculation, a strong signal derived from HIF-1α protein was detected in the liver sections prepared at 2 days after tumor inoculation (Figure 3i).

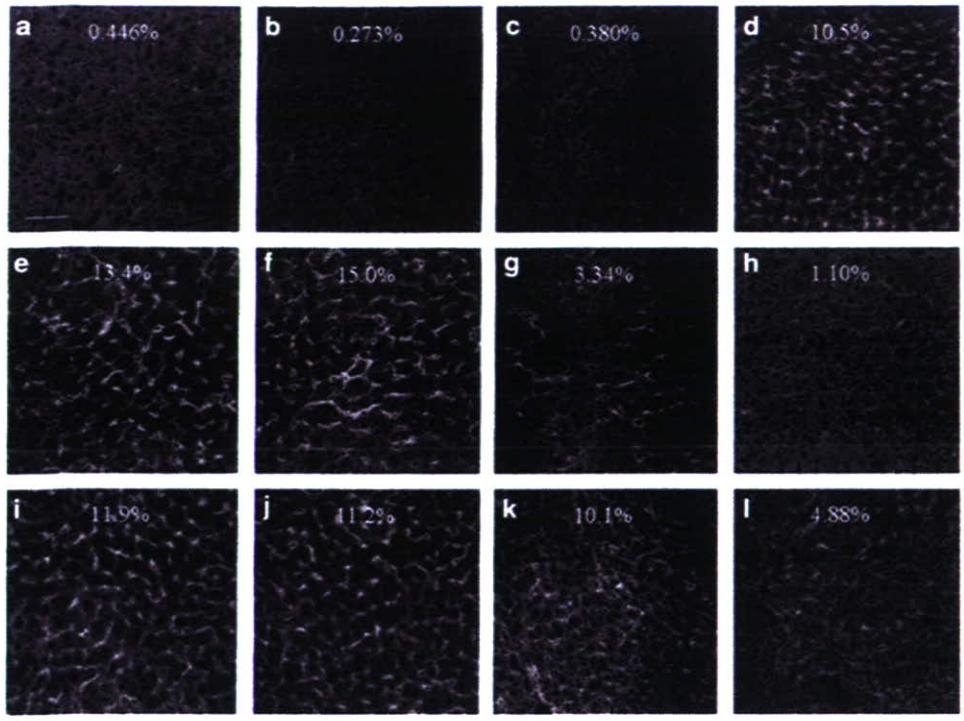


**Figure 3** Hypoxia-inducible factor-1α (HIF-1α) expression in the liver of tumor-bearing mice. Some mice were untreated (**a**) or received plasmid DNA (pDNA) only (**b**). The sham operation group (**c**) received only an intraportal injection of Hank's balanced salt solution (HBSS) solution without tumor cells. At 5 days after tumor inoculation via the portal vein, mice were untreated (**d**) or received an intravenous injection of control pDNA (**e**), pshGFP (green fluorescent protein) (**f**) or pDNA expressing shRNA targeting HIF-1α (pshHIF-1α) (**g**). At 2 days after pDNA administration, liver samples were collected and subjected to immunostaining for HIF-1α. The sham operation group received only an intraportal injection of HBSS solution without tumor cells (**h**). At 3 days before tumor inoculation via the portal vein, mice were untreated (**i**) or received an intravenous injection of control pDNA (**j**), pshGFP (**k**) or pshHIF-1α (**l**). At 2 days after tumor inoculation, liver samples were collected and subjected to immunostaining for HIF-1α. Scale bar = 50 μm. Numbers in the images represent the relative area of HIF-1α expression (green signal) to the total area. See online version for color figure.

pshHIF-1α administrated before tumor inoculation suppressed the induction of HIF-1α expression by tumor inoculation (Figure 3l). Administration of irrelevant pDNAs did not change the expression level of HIF-1α in the liver (Figures 3j and k). Quantification of the relative areas of the HIF-1α expression (green signal) to the total area in the images indicated that pre-administration of pshHIF-1α reduced HIF-1α expression to about 50% of the other tumor-inoculated groups.

### *Location of HIF-1α expression in the tumor-inoculated liver relative to tumor cells*

To visualize Colon26 cells in the liver, Colon26 cells transfected with pDsRed2-N1 were inoculated into the portal vein of mice. Immunofluorescent staining for HIF-1α was performed at 2 days after tumor inoculation to investigate the location of HIF-1α expression relative to tumor cells (Figures 4a–d). DsRed-labeled Colon26 cells were found in some liver sections, and almost all of these cells were surrounded by liver cells expressing an increased level of HIF-1α (Figures 4a and b). Some liver cells not close to Colon26 cells also showed a high HIF-1α expression (Figure 4c), but most other liver cells hardly expressed the protein (Figure 4d). These results suggest that tumor cells entrapped in the hepatic capillaries is closely associated with the increased expression of HIF-1α in the surrounding liver cells.

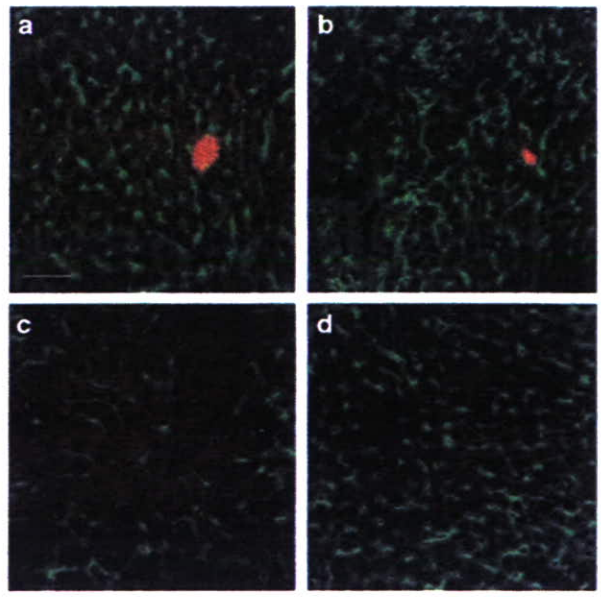


**Figure 4** Location of hypoxia-inducible factor-1α (HIF-1α) expression in the tumor-bearing liver relative to tumor cells. At 2 days after tumor inoculation, liver samples were collected and subjected to immunostaining for HIF-1α. Red signals represent Colon26 cells expressing DsRed, and green signals represent HIF-1α protein. Representative images of liver sections positive (**a**, **b**) or negative (**c**, **d**) for DsRed-labeled Colon26 cells are indicated. Scale bar = 50 μm.

### *Induction of MMP-2 and -9 expression in the liver by tumor inoculation via the portal vein*

To evaluate the effect of tumor inoculation via the portal vein on the MMP expression in the liver, the amount of MMP in liver homogenate was measured by gelatin zymography 8 days after tumor inoculation (Figure 5a). As we have reported previously, MMP-2 and -9 activities in the homogenate of tumor-inoculated liver was higher than that of the untreated group. A hydrodynamic delivery of control pDNA or pshGFP 5 days after tumor inoculation had little or no effect on both types of MMP activity. No significant increase in the MMP activity was detected in the liver homogenate of sham-operated mice or mice that received only pDNA. Intravenous injection of pshHIF-1α by the hydrodynamics-based procedure 5 days after tumor inoculation clearly reduced the MMP-9 gelatinolytic activity in the liver of tumor-bearing mice compared with the other tumor-inoculated group. Less, but detectable, reduction was also observed in the MMP-2 activity.

To assess the effect of HIF-1α expression in normal cells on MMP production, pshHIF-1α was administered 3 days before tumor inoculation. Gelatin zymography was performed at 3 days after tumor inoculation (Figure 5b). At this time point, the sham operation group showed slightly increased MMP-9 activity compared with naïve mice. Although the increase in MMP-9 expression level in the liver at this time was smaller than that detected at 8 days after tumor inoculation, the homogenate of tumor-bearing liver showed a higher MMP-9 activity than the other tumor-free groups. Pretreatment of pshHIF-1α reduced MMP-9 induction by tumor inoculation, while preinjection of control pDNA and

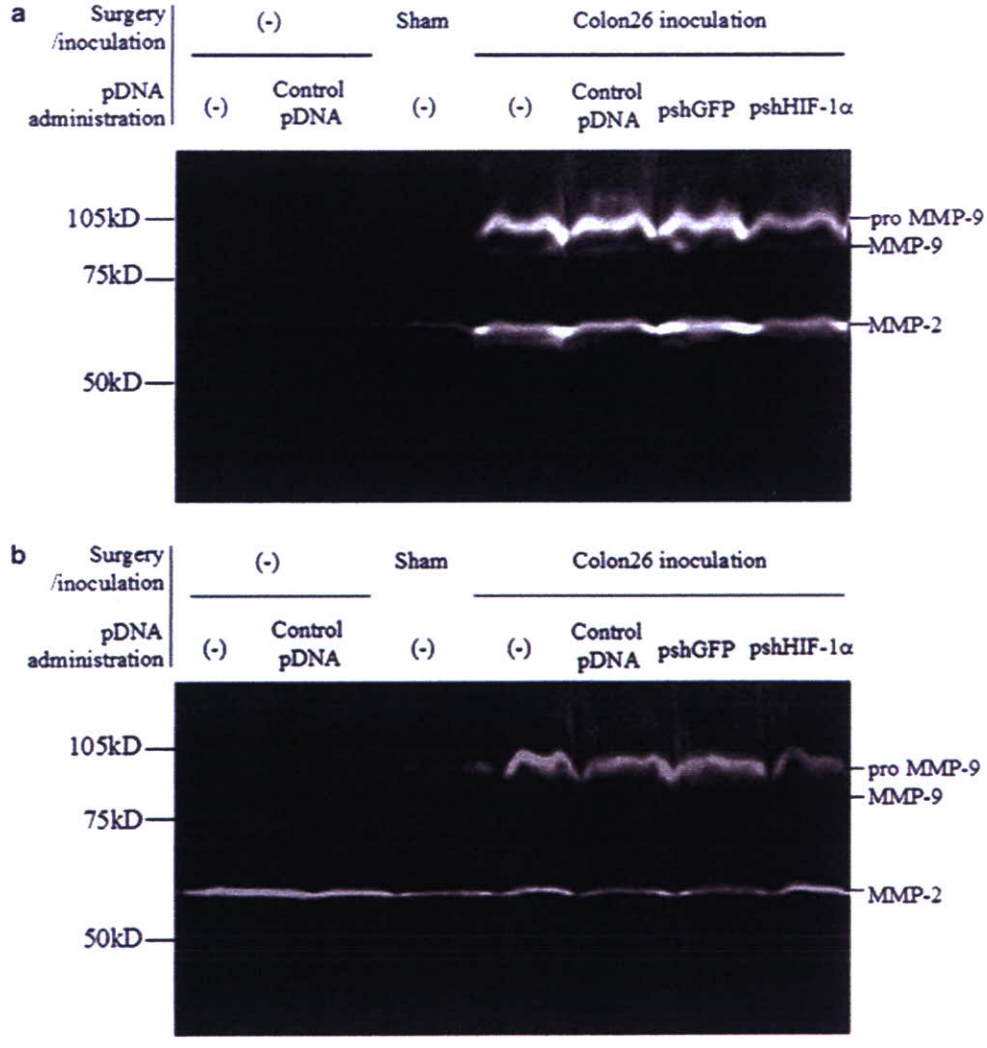


**Figure 5** Gelatin zymography performed on liver samples. (**a**) At 5 days after tumor inoculation via the portal vein, mice received an intravenous injection of control plasmid DNA (pDNA), pshGFP (green fluorescent protein) or pDNA expressing shRNA targeting HIF-1α (pshHIF-1α). The sham operation group received only an intraportal injection of Hank's balanced salt solution (HBSS) solution without tumor cells. At 3 days after pDNA administration, liver samples were collected and subjected to gelatin gel zymography. Four mice of each group were used to analyze the matrix metalloproteinase (MMP) expression, and typical results are shown. (**b**) At 3 days before tumor inoculation via the portal vein, mice received an intravenous injection of control pDNA, pshGFP or pshHIF-1α. The sham operation group received only an intraportal injection of HBSS solution without tumor cells. At 3 days after tumor inoculation, liver samples were collected and subjected to gelatin gel zymography. Four mice of each group were used to analyze the MMP expression, and typical results are shown.

pshGFP had little effect on MMP-9 induction in the liver following tumor inoculation. We did not observe any obvious difference in MMP-2 production between tumor-free and tumor-bearing groups.

### *Suppression of metastatic tumor growth in the liver by pshHIF-1α*

Figure 6a shows the tumor cell number in the liver, which was evaluated by measuring tumor-derived luciferase activities at 1 week after pDNA administration (Figure 6a). Mice were inoculated with Colon26 cells into the portal vein, and each pDNA was injected into the tail vein with 5-day interval. Control pDNA or pshGFP hardly reduced the number of tumor cells, while pshHIF-1α significantly ($P<0.05$) reduced the number to about, on average, 1–2% of the other groups. Many large tumor nodules were found in the frozen liver sections of mice receiving control pDNA (Figure 6c). In a quite contrast, much small and few tumor nodules were detected in the sections of mice receiving pshHIF-1α (Figure 6d). These hematoxylin and eosin-stained sections strongly support the quantitative results of metastatic tumor growth estimated using the luciferase activity of Colon26/Luc cells (Figure 6a).

Next, we investigated the effect of preadministration of pshHIF-1α on the growth of tumor cells in the liver by estimating the tumor cell number 12 days after tumor inoculation (Figure 6b). As a result, pshHIF-1α preadministration 3 days before tumor inoculation significantly reduced the number of tumor cells in the liver 12 days after tumor inoculation compared with the groups that were untreated or given pDNA. On average,

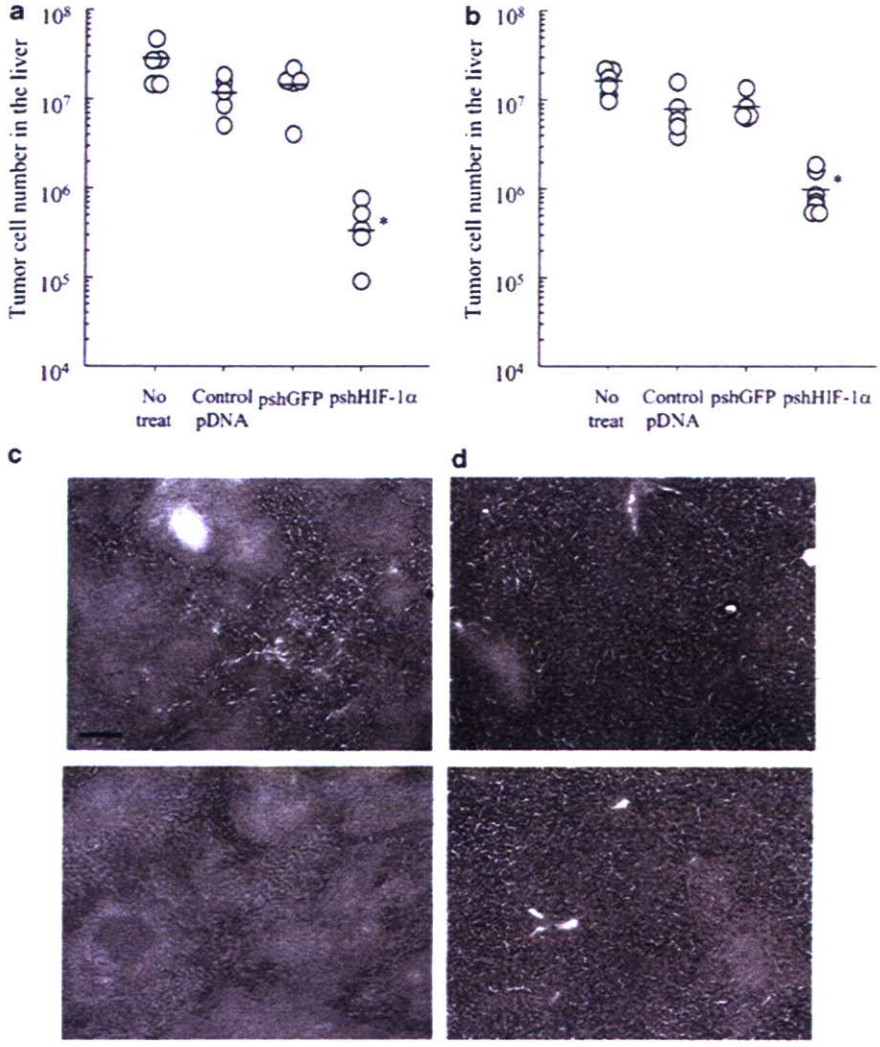


**Figure 6** Number of Colon26/Luc cells in mouse liver 12 days after tumor inoculation. (**a**) At 5 days after tumor inoculation via the portal vein, mice received an intravenous injection of control plasmid DNA (pDNA), pshGFP (green fluorescent protein) or pDNA expressing shRNA targeting HIF-1α (pshHIF-1α). At 7 days after pDNA administration, liver samples were collected and the number of tumor cells was evaluated by measuring luciferase activities derived from Colon26/Luc cells. Open circles (○) indicate the tumor cell number in the liver of individual mice. Bars indicate the average tumor cell number of each group ($n=5$). *$P<0.05$ for Student's *t*-test versus untreated group. (**b**) At 3 days before tumor inoculation via the portal vein, mice received an intravenous injection of control pDNA, pshGFP or pshHIF-1α. At 12 days after tumor inoculation, liver samples were collected and the number of tumor cells was evaluated by measuring luciferase activities derived from Colon26/Luc cells. Open circles (○) indicate the tumor cell number in the liver of individual mice. Bars indicate the average tumor cell number of each group of at least five mice. *$P<0.05$ for Student's *t*-test versus untreated group. (**c**, **d**) Hematoxylin and eosin-stained liver sections of tumor-bearing mice receiving (**c**) control pDNA or (**d**) pshHIF-1α at 7 days after tumor inoculation. Scale bar = 200 μm. See online version for color figure.

preadministration of pshHIF-1α reduced the number of tumor cells to about 10% of other groups. The degree of reduction in the number of tumor cells by pshHIF-1α administered before tumor inoculation was about 5- to 10-fold less than that of pshHIF-1α administered after tumor inoculation.

## Discussion

HIF-1α expression and subsequent HIF-1 activation in cancer cells play important roles in cancer progression by controlling the gene expression related to cancer cell proliferation, apoptosis and metastasis.[9] In the present study, we demonstrated that HIF-1α expression in normal hepatic cells is also increased by tumor cells entering the liver via the portal vein and that such HIF-1α expression aggravates tumor growth. Our results indicate the possibility of a novel therapeutic strategy for inhibiting metastatic tumor growth by silencing the HIF-1α expression in both normal and tumor cells.

Suppression of nuclear accumulation of HIF-1α by pshHIF-1α (Figure 1) was followed by inhibition of HIF-1-dependent transcription activities (Figure 2). In the experiment using pLuc-HRE, pshHIF-1α suppressed the transcription activity to almost the basal level in both Colon26 and B16-BL6 cells. Such an efficient inhibitory effect on luciferase expression might be because pLuc-HRE was co-transfected with pshHIF-1α, by which both pDNAs were delivered to the same cells. On the other hand, the suppressive effect of pshHIF-1α on VEGF production from B16-BL6 cells was much greater than that from Colon26 cells. Two factors may explain the difference in the efficiency of the inhibitory effect on VEGF production between B16-BL6 cells and Colon26 cells. One is the transfection efficiency of the pshHIF-1α. By using pDNA expressing enhanced green fluorescent protein (EGFP), we found that the transfection efficiency to B16-BL6 and Colon26 cells was about 80–90 and 70–80%, respectively, at 24 h after transfection (Y Takahashi *et al.*, unpublished data). Therefore, the difference in transfection efficiency between B16-BL6 and Colon26 cells may be one reason for the difference in suppressive effect on VEGF production by pshHIF-1α. The other reason for the difference in suppression in the two cell lines could be the contribution of HIF-1-dependent VEGF production to the total VEGF production. Other hypoxia-inducible transcriptional factors, such as HIF-2, are also known to be activated by $CoCl_2$ and increased HIF-2 expression might result in VEGF expression.[19]

When tumor cells were inoculated via portal vein, HIF-1α protein expression was increased in tumor-bearing liver (Figure 3). Inoculation of DsRed-labeled Colon26 cells clearly demonstrated that liver cells close to the tumor cells expressed HIF-1α at a high level (Figure 4). Oxygen concentration-dependent and -independent pathways might be considered as the mechanism for such an increase in HIF-1α expression. When tumor cells are inoculated via the portal vein, tumor cells are first arrested in small vessels, followed by extravasation, invasion of tissues and proliferation of tumor cells.[3] Therefore, blood flows would be, at least transiently, hindered by tumor cells, which could result in a reduction in the oxygen supply. In addition to hypoxia, other processes such as growth factor stimulation and cytokine stimulation are reported to increase HIF-1α expression and activate HIF-1-dependent transcription.[9,20] When tumor cells metastasize to the liver, expression of these secretary proteins might be induced and result in increased HIF-1α expression.

To distinguish the role of HIF-1α expressed in tumor cells from that in normal liver cells, pshHIF-1α was administered 3 days before tumor inoculation. As pDNA injected into the systemic circulation is very quickly degraded by nucleases and cleared by Kupffer and sinusoidal endothelial cells,[21] pDNA injected would have hardly any effects on the expression level of HIF-1α in Colon26/Luc cells. On the other hand, when pshHIF-1α was administered after tumor inoculation, pshHIF-1α might be delivered to both tumor and liver cells.[18] Therefore, pshHIF-1α administered before tumor inoculation might have been delivered only to normal cells in the liver, while pshHIF-1α administered after tumor inoculation might have been delivered to both tumor and normal cells in the liver.

In a previous study, we reported that Colon26 cell inoculation via the portal vein increased MMP-9 expression in the liver.[22] Elezkurtaj *et al.*[23] demonstrated that intrasplenic inoculation of CT-26 colon carcinoma cells, which form experimental liver metastases, increased MMP-2 and -9 expressions in liver tissue. In agreement with these results, we have found that MMP-9 is generated mainly from host cells, not the inoculated tumor cells (Y Takahashi *et al.*, unpublished data). There are some published papers reporting that MMP-9 expression is directly or indirectly regulated by HIF-1.[24–26] Therefore, we hypothesized that increased HIF-1 transcription activity in normal cells in the liver contributes to MMP-9 production induced by tumor cell inoculation. Intravenous administration of pshHIF-1α was effective in reducing the expression of MMP-9 after tumor inoculation, which indicates that HIF-1 expression in tumor cells and normal cells in the liver might play an important role in MMP-9 production. Moreover, administration of pshHIF-1α before tumor inoculation was found to be also effective in reducing the amount of MMP-9 in the liver. This result reinforces the hypothesis that normal cells in the liver, not tumor cells, are the major producer of MMP-9 and that MMP-9 expression is regulated by HIF-1. Although its role in metastatic tumor cell growth is still unclear, increased MMP expression is frequently accompanied by tumor metastasis and suppression of MMP expression could be used as a growth inhibitory treatment to prevent tumor metastasis.[23,27,28]

When pshHIF-1α was administered to tumor-bearing mice by the hydrodynamics-based procedure, a significant reduction in the number of tumor cells was observed (Figure 6a). This result indicates that HIF-1α expression in either tumor cells or hepatic normal cells or in both types of cells plays an important role in tumor progression. A histological study of the liver sections confirmed that the administration of pshHIF-1α significantly reduced the metastatic tumor growth in the liver (Figures 6c and d). Preadministration of pshHIF-1α reduced the tumor cell number in the liver at 12 days after tumor inoculation compared with the other groups (Figure 6b). This result implies that HIF-1α expression in the normal cells in the liver might play an important role in tumor cell growth in the liver, although the reduction

in the tumor cell number was modest compared with the case where the pshHIF-1α was administered after tumor inoculation. As demonstrated in our previous study, hydrodynamic delivery of pDNA can deliver pDNA to tumor cells in the liver. Moreover, we and other groups have reported that intratumoral expression of HIF-1α helps cancer cell survival and proliferation as well as angiogenesis and cancer metastasis. Therefore, hydrodynamic administration of pshHIF-1α could suppress HIF-1α expression in tumor cells, which might also act as an inhibitory treatment to prevent tumor progression. When HIF-1α expression is increased in normal cells, it might result in upregulation of genes that can assist tumor cell growth and progression. In the present study, we focused on MMP-9 as an HIF-1-dependent tumor supportive protein produced from normal cells. Normal cells, including hepatocytes, have significantly fewer genetic mutations than cancer cells. Therefore, inhibiting the increase in HIF-1α expression in hepatocytes would have less chance of inducing resistance to treatment.

In conclusion, this study suggests that HIF-1α expression is increased in normal liver cells as well as cancerous cells, and HIF-1α expression plays an important role in tumor progression. RNAi of HIF-1 is an effective strategy for inhibiting tumor cell growth, and both tumor and normal cells can be targets for RNAi-based anticancer treatment.

## Materials and methods

### *Plasmid DNA*

Short hairpin-expressing pDNAs targeting GFP or HIF-1α were constructed from piGENE hU6 vector (iGENE Therapeutics, Tsukuba, Japan) as described previously.[18] Target sites in GFP and murine HIF-1α genes are as follows: GFP, 5′-GGCTACGTCCAGGAGCGCA-3′ and HIF-1α, 5′-GACACAGCCTCGATATGAA-3′. These pDNAs transcribe a stem-loop-type RNA with a loop sequence of ACGUGUGCUGUCCGU. In a previous study, we confirmed that transfection of pshHIF-1α suppresses the mRNA expression of HIF-1α in cultured cells.[13] piGENE hU6 vector, which transcribes a non-related sequence of RNA with partial duplex formation, was used as a control pDNA throughout the present study.

pDsRed2-N1 encoding red fluorescent protein Dsred2 was purchased from BD Biosciences Clontech (Palo Alto, CA, USA). pGL4.74[hRluc/TK] (phRL-TK) encoding sea pansy luciferase under the control of herpes simplex virus TK promoter was purchased from Promega (Madison, WI, USA). A HRE reporter plasmid encoding firefly luciferase (pLuc-HRE) was generated by subcloning nine copies of the HRE (5′-TACGTGCTGC-3′) from mouse erythropoietin enhancer into *Bgl*II/*Hin*dIII site of pLuc-MCS plasmid (Stratagene, La Jolla, CA, USA).

Each pDNA was amplified in the DH5α strain of *Escherichia coli* and purified by using a Qiagen Endofree Plasmid Giga Kit (Qiagen GmbH, Hilden, Germany).

### *Cell culture*

A murine colon carcinoma cell line Colon26, obtained from the Cancer Chemotherapy Center of the Japanese Foundation for Cancer Research (Tokyo, Japan), and Colon26 cells that stably express firefly luciferase (Colon26/Luc)[29] were cultured in RPMI 1640 medium supplemented with 10% fetal bovine serum (FBS) and penicillin/streptomycin/L-glutamine at 37 °C and 5% $CO_2$. A murine melanoma cell line B16-BL6 cells[30], obtained from the Cancer Chemotherapy Center of the Japanese Foundation for Cancer Research, were cultured in Dulbecco's modified Eagle's minimum essential medium (DMEM; Nissui Pharmaceutical, Tokyo, Japan) supplemented with 10% FBS and penicillin/streptomycin/L-glutamine at 37 °C and 5% $CO_2$. To mimic hypoxic conditions and induce HIF-1α protein expression, cells were incubated with the culture medium supplemented with 100 μM $CoCl_2$.[31]

### In vitro *transfection*

Tumor cells were plated on culture plates. After an overnight incubation, transfection of pDNA was carried out using Lipofectamine 2000 (Invitrogen, Carlsbad, CA, USA) according to the manufacturer's instructions. In brief, 1 μg pDNA was mixed with 3 μg Lipofectamine 2000 at a final concentration of 2 μg pDNA $ml^{-1}$ dissolved in OPTI-MEM I (Invitrogen). The resulting complex was added to the cells and the cells were incubated with the complex for 4 h. Cells were washed with PBS and further incubated with the culture medium supplemented with or without 100 μM $CoCl_2$ for the indicated periods.

### *Detection of HIF-1α protein expression by western blotting and ELISA*

At 24 h after transfection, total proteins were collected from Colon26 and B16-BL6 cells. For total protein extraction, cells were lysed in a lysis buffer containing 50 mM Tris (pH 7.4), 1% NP40, 0.25% Na-deoxycholate, 0.1% SDS, 150 mM NaCl, 1 mM EDTA, 1 mM PMSF, 1 mM NaF and 0.2% Sigma protease inhibitor cocktail (Sigma Aldrich, St Louis, MO, USA). The lysate was centrifuged at 13 000 *g* for 20 min at 4 °C and the supernatant was collected and used as a protein sample. Protein concentrations were determined using a Proteostain Protein Quantification Kit (Dojindo Molecular Technologies Inc., Tokyo, Japan).

For western blotting, 50 μg protein was diluted with a loading buffer, denatured at 95 °C for 3 min, and resolved by SDS-polyacrylamide gel electrophoresis (SDS-PAGE) (6.5% polyacrylamide) and transferred to a polyvinylidene fluoride membrane (Immobilon-P; Millipore Corp., Bedford, MA, USA) by semidry blotting with Transblot SD (Bio-Rad, Hercules, CA, USA). To avoid nonspecific binding, the membrane was incubated in 5% bovine serum albumin. Then HIF-1α protein was detected by a primary monoclonal mouse antibody against HIF-1α (1:500; Novus Biologicals, Littleton, CO, USA) and a secondary peroxidase-conjugated rabbit anti-mouse IgG antibody (1:2000; Amersham Biosciences Inc., Piscataway, NJ, USA). Protein bands were visualized by chemiluminescence on the ECL Plus protein detection system (Amersham Biosciences).

Concentrations of HIF-1α in the samples from tumor cells treated with or without $CoCl_2$ were measured by an ELISA kit (DuoSet IC; R&D Systems, Minneapolis, MN, USA) according to manufacturer's protocol.

### *HIF-1-dependent reporter gene expression assay*

Tumor cells seeded on culture plates were transfected with pLuc-HRE (0.8 μg $ml^{-1}$), phRL-TK (0.2 μg $ml^{-1}$) and a control pDNA, pshHIF-1α or pshGFP (1 μg $ml^{-1}$) using Lipofectamine 2000 as described above. At 4 h after transfection, cells were washed with PBS and further incubated with the culture medium with or without 100 μM $CoCl_2$ for an additional 20 h. Then cells were lysed using Promega passive lysis buffer (Promega). Samples were mixed with dual-luciferase reporter system (Promega) and the chemiluminescence produced was measured in a luminometer (Lumat LB9507; EG and G Berthold, Bad Wildbad, Germany). The results were calculated as the activity of firefly luciferase relative to that of sea pansy luciferase to correct for differences in transfection efficiency. The ratios of $CoCl_2$-treated cells were normalized to give *x*-fold values relative to those of the corresponding untreated group.

### *Animals*

Four-week-old male BALB/c mice (approximately 20 g body weight), purchased from Shizuoka Agricultural Cooperative Association (Shizuoka, Japan), were used in all experiments. All animal experiments were conducted in accordance with the principles and procedures outlined in the US National Institutes of Health Guide for the Care and Use of Laboratory Animals. The protocols for animal experiments were approved by the Animal Experimentation Committee of the Graduate School of Pharmaceutical Sciences of Kyoto University.

### *Hepatic metastasis of tumor cells*

Colon26/Luc cells in an exponential growth phase were harvested by trypsinization and suspended in Hank's balanced salt solution (HBSS; Nissui Pharmaceutical). Under ether anesthesia, a midline abdominal incision was made to expose the portal vein, and $1 \times 10^5$ Colon26/Luc cells were injected into the portal vein. Then the opening was sutured and mice were allowed to recover. At 5 days after tumor inoculation, mice received an intravenous injection of pDNA at a dose of 2.5 mg $kg^{-1}$ body weight. The intravenous injection was performed by the hydrodynamics-based procedure where pDNA dissolved in saline in a volume of 8% of the body weight was injected into the tail vein within less than 5 s using a 26-gauge needle.[32]

To evaluate the effect of HIF-1α expression in normal liver cells on the growth of tumor cells in the liver, mice received a hydrodynamic delivery of pDNA, followed by inoculation of tumor cells into the portal vein after an interval of 3 days.

To visualize the location of Colon26 cells in the liver, Colon26 cells labeled with a red fluorescent protein, DsRed, were used instead of Colon26/Luc cells. DsRed2-labeled Colon26 cells were prepared by transfecting cells with pDsRed2-N1, and inoculated into mice 24 h after transfection.

### *Immunofluorescent staining of HIF-1α*

To visualize HIF-1α expression in cultured cells, immunofluorescent staining of HIF-1α was carried out. At 24 h after transfection, cells were fixed with 4% paraformaldehyde in PBS. The cell membrane was permeabilized by PBS containing 0.1% Triton X-100. After blocking with 10% FBS in PBS, cells were incubated with a monoclonal mouse antibody against HIF-1α (1:500; Novus Biologicals). After washing, Alexa Fluor 488 goat anti-mouse secondary antibody (1:600; Molecular Probes, Invitrogen) was added. Nuclear staining was performed using propidium iodide staining solution (50 μg $ml^{-1}$ propidium iodide and 1 μg $ml^{-1}$ RNase A in PBS). Slides were prepared using a SlowFade Antifade Kit (Molecular Probes). Samples were examined using a confocal laser microscope (MRC-1024; Bio-Rad).

For the detection of HIF-1α expression in the liver, mice under ether anesthesia were euthanized by cutting the vena cava, and the liver was gently infused with 2 ml saline through the portal vein to remove the remaining blood in the organ. The liver was then placed in Tissue-Tek OCT embedding compound (Sakura Finetechnical Co Ltd, Tokyo, Japan), frozen in liquid nitrogen, and stored in 2-methyl butanol at −80 °C until use. Frozen liver sections (8 μm thick) were obtained with a cryostat (Jung CM 3000; Leica Microsystems AG, Wetzlar, Germany) using a routine procedure. Sections were stained with HIF-1α-specific antibody by the same procedure as cultured cells except for the blocking process. Liver sections were blocked using the Vector M.O.M Immunodetection Kit (Vector Laboratories, Burlingame, CA, USA). Sections were examined using a confocal laser microscope. Relative areas of the HIF-1α expression (green signal) to the total area in the images were quantitatively analyzed by using a BZ-Analyzer software (KEYENCE, Osaka, Japan).

### *Gelatin zymography*

At 3 or 8 days after tumor inoculation, mice under ether anesthesia were euthanized by cutting the vena cava. The liver was gently infused with 2 ml saline through the portal vein to remove the remaining blood. The liver was excised and homogenized in 5 ml $g^{-1}$ lysis buffer (0.1 M Tris (pH 7.8), 0.05% Triton-X-100). The homogenate was centrifuged at 13 000 *g* for 20 min at 4 °C, then the supernatant was collected. For the measurement of gelatinase activity, 500 μg protein was electrophoresed under non-reducing conditions on 10% SDS-polyacrylamide gel containing 0.1% gelatin. Gels were washed twice for 30 min in 2.5% Triton X-100 and once for 30 min in 10 mM Tris-HCl (pH 8.0) and incubated overnight in 50 mM Tris-HCl (pH 8.0) containing 10 mM $CaCl_2$ and 10 nM $ZnCl_2$. The gels were then stained with 0.2% Coomasie brilliant blue and destained in 5% methanol and 7% acetic acid.

### *VEGF ELISA assay*

To determine VEGF production in culture supernatants *in vitro*, tumor cells seeded on culture plates were transfected as described above and supernatants were collected for ELISA 48 h after the transfection. VEGF protein levels in the supernatant were measured using mouse VEGF-specific ELISA (Quantikine; R&D systems).

### *Inhibitory effect of pshHIF-1α on tumor growth in the liver*

At 12 days after tumor inoculation, mice were euthanized by cervical dislocation and the liver was excised and homogenized in a lysis buffer (0.1 M Tris (pH 7.8), 0.05% Triton X-100, 2 mM EDTA), and centrifuged at

13 000 *g* for 20 min at 4 °C. The supernatant was mixed with a luciferase assay buffer (Picagene; Toyo Ink, Tokyo, Japan), and the light produced was measured with a luminometer (Lumat LB 9507). The luciferase activity of the liver was converted to the number of Colon26/Luc cells using a regression line as previously reported.[29] Different sets of mice were used for the histological evaluation of tumor-bearing livers. At 12 days after tumor inoculation, frozen liver sections were made as described above and stained with hematoxylin and eosin, followed by an examination using a microscope (Biozero BZ-8000; KEYENCE).

### *Statistical analysis*

Experiments were performed at least in duplicate, and a typical set of data was indicated. Differences were statistically evaluated by Student's *t*-test. A *P*-value of less than 0.05 was considered to be statistically significant.

## Acknowledgements

This study was supported in part by Grants-in-Aid for Scientific Research from the Ministry of Education, Science, Sports, and Culture of Japan, by grants from the Ministry of Health, Labour and Welfare of Japan and by a Grant-in-Aid for Exploratory Research from the Japan Society for the Promotion of Sciences.

## References

1 Fidler IJ. Critical determinants of metastasis. *Semin Cancer Biol* 2002; **12**: 89–96.
2 Weigelt B, Peterse JL, van't Veer LJ. Breast cancer metastasis: markers and models. *Nat Rev Cancer* 2005; **5**: 591–602.
3 Engers R, Gabbert HE. Mechanisms of tumor metastasis: cell biological aspects and clinical implications. *J Cancer Res Clin Oncol* 2000; **126**: 682–692.
4 Olaso E, Santisteban A, Bidaurrazaga J, Gressner AM, Rosenbaum J, Vidal-Vanaclocha F. Tumor-dependent activation of rodent hepatic stellate cells during experimental melanoma metastasis. *Hepatology* 1997; **26**: 634–642.
5 Liotta LA, Kohn EC. The microenvironment of the tumour–host interface. *Nature* 2001; **411**: 375–379.
6 Wang GL, Semenza GL. General involvement of hypoxia-inducible factor 1 in transcriptional response to hypoxia. *Proc Natl Acad Sci USA* 1993; **90**: 4304–4308.
7 Wenger RH. Cellular adaptation to hypoxia: $O_2$-sensing protein hydroxylases, hypoxia-inducible transcription factors, and $O_2$-regulated gene expression. *FASEB J* 2002; **16**: 1151–1162.
8 Salceda S, Caro J. Hypoxia-inducible factor 1alpha (HIF-1alpha) protein is rapidly degraded by the ubiquitin-proteasome system under normoxic conditions. Its stabilization by hypoxia depends on redox-induced changes. *J Biol Chem* 1997; **272**: 22642–22647.
9 Semenza GL. Targeting HIF-1 for cancer therapy. *Nat Rev Cancer* 2003; **3**: 721–732.
10 Zhong H, De Marzo AM, Laughner E, Lim M, Hilton DA, Zagzag D *et al*. Overexpression of hypoxia-inducible factor 1alpha in common human cancers and their metastases. *Cancer Res* 1999; **59**: 5830–5835.
11 Talks KL, Turley H, Gatter KC, Maxwell PH, Pugh CW, Ratcliffe PJ *et al*. The expression and distribution of the hypoxia-inducible factors HIF-1alpha and HIF-2alpha in normal human tissues, cancers, and tumor-associated macrophages. *Am J Pathol* 2000; **157**: 411–421.
12 Li L, Lin X, Staver M, Shoemaker A, Semizarov D, Fesik SW *et al*. Evaluating hypoxia-inducible factor-1alpha as a cancer therapeutic target via inducible RNA interference *in vivo*. *Cancer Res* 2005; **65**: 7249–7258.
13 Takahashi Y, Nishikawa M, Takakura Y. Suppression of tumor growth by intratumoral injection of short hairpin RNA-expressing plasmid DNA targeting beta-catenin or hypoxia-inducible factor 1alpha. *J Control Release* 2006; **116**: 90–95.
14 Elbashir SM, Harborth J, Lendeckel W, Yalcin A, Weber K, Tuschl T. Duplexes of 21-nucleotide RNAs mediate RNA interference in cultured mammalian cells. *Nature* 2001; **411**: 494–498.
15 Brummelkamp TR, Bernards R, Agami R. A system for stable expression of short interfering RNAs in mammalian cells. *Science* 2002; **296**: 550–553.
16 McCaffrey AP, Meuse L, Pham T-TT, Conklin DS, Hannon GJ, Kay MA. RNA interference in adult mice. *Nature* 2002; **418**: 38–39.
17 Song E, Lee SK, Wang J, Ince N, Ouyang N, Min J *et al*. RNA interference targeting Fas protects mice from fulminant hepatitis. *Nat Med* 2003; **9**: 347–351.
18 Takahashi Y, Nishikawa M, Kobayashi N, Takakura Y. Gene silencing in primary and metastatic tumors by small interfering RNA delivery in mice: quantitative analysis using melanoma cells expressing firefly and sea pansy luciferases. *J Control Release* 2005; **105**: 332–343.
19 Carroll VA, Ashcroft M. Role of hypoxia-inducible factor (HIF)-1alpha versus HIF-2alpha in the regulation of HIF target genes in response to hypoxia, insulin-like growth factor-I, or loss of von Hippel–Lindau function: implications for targeting the HIF pathway. *Cancer Res* 2006; **66**: 6264–6270.
20 Mazure NM, Brahimi-Horn MC, Berta MA, Benizri E, Bilton RL, Dayan F *et al*. HIF-1: master and commander of the hypoxic world. A pharmacological approach to its regulation by siRNAs. *Biochem Pharmacol* 2004; **68**: 971–980.
21 Kawabata K, Takakura Y, Hashida M. The fate of plasmid DNA after intravenous injection in mice: involvement of scavenger receptors in its hepatic uptake. *Pharm Res* 1995; **12**: 825–830.
22 Nishikawa M, Tamada A, Hyoudou K, Umeyama Y, Takahashi Y, Kobayashi Y *et al*. Inhibition of experimental hepatic metastasis by targeted delivery of catalase in mice. *Clin Exp Metastasis* 2004; **21**: 213–221.
23 Elezkurtaj S, Kopitz C, Baker AH, Perez-Cantó A, Arlt MJ, Khokha R *et al*. Adenovirus-mediated overexpression of tissue inhibitor of metalloproteinases-1 in the liver: efficient protection against T-cell lymphoma and colon carcinoma metastasis. *J Gene Med* 2004; **6**: 1228–1237.
24 Krishnamachary B, Berg-Dixon S, Kelly B, Agani F, Feldser D, Ferreira G *et al*. Regulation of colon carcinoma cell invasion by hypoxia-inducible factor 1. *Cancer Res* 2003; **63**: 1138–1143.
25 Shi YF, Fong CC, Zhang Q, Cheung PY, Tzang CH, Wu RS *et al*. Hypoxia induces the activation of human hepatic stellate cells LX-2 through TGF-beta signaling pathway. *FEBS Lett* 2007; **581**: 203–210.
26 Stuelten CH, DaCosta Byfield S, Arany PR, Karpova TS, Stetler-Stevenson WG, Roberts AB. Breast cancer cells induce stromal fibroblasts to express MMP-9 via secretion of TNF-alpha and TGF-beta. *J Cell Sci* 2005; **118**: 2143–2153.
27 Waas ET, Wobbes T, Lomme RM, DeGroot J, Ruers T, Hendriks T. Matrix metalloproteinase 2 and 9 activity in patients with colorectal cancer liver metastasis. *Br J Surg* 2003; **90**: 1556–1564.
28 Lakka SS, Rajan M, Gondi C, Yanamandra N, Chandrasekar N, Jasti SL *et al*. Adenovirus-mediated expression of antisense MMP-9 in glioma cells inhibits tumor growth and invasion. *Oncogene* 2002; **21**: 8011–8019.
29 Kuramoto Y, Nishikawa M, Hyoudou K, Yamashita F, Hashida M. Inhibition of peritoneal dissemination of tumor cells by single dosing of phosphodiester CpG oligonucleotide/cationic liposome complex. *J Control Release* 2006; **115**: 226–233.

30 Poste G, Doll J, Hart IR, Fidler IJ. *In vitro* selection of murine B16 melanoma variants with enhanced tissue-invasive properties. *Cancer Res* 1980; **40**: 1636–1644.
31 Gray MJ, Zhang J, Ellis LM, Semenza GL, Evans DB, Watowich SS *et al*. HIF-1alpha, STAT3, CBP/p300 and Ref-1/APE are components of a transcriptional complex that regulates Src-dependent hypoxia-induced expression of VEGF in pancreatic and prostate carcinomas. *Oncogene* 2005; **24**: 3110–3120.
32 Liu F, Song Y, Liu D. Hydrodynamics-based transfection in animals by systemic administration of plasmid DNA. *Gene Ther* 1999; **6**: 1258–1266.

*Int. J. Cancer:* **121**, 401–406 (2007)


# Improved anti-cancer effect of interferon gene transfer by sustained expression using CpG-reduced plasmid DNA

**Hiroki Kawano[1], Makiya Nishikawa[1], Masaru Mitsui[1], Yuki Takahashi[1], Keiko Kako[1], Kiyoshi Yamaoka[1], Yoshihiko Watanabe[2] and Yoshinobu Takakura[1]***

[1]*Department of Biopharmaceutics and Drug Metabolism, Graduate School of Pharmaceutical Sciences, Kyoto University, Sakyo-ku, Kyoto, Japan*
[2]*Department of Molecular Microbiology, Graduate School of Pharmaceutical Sciences, Kyoto University, Sakyo-ku, Kyoto, Japan*

**Plasmid DNA (pDNA) expressing mouse interferon (IFN)-β or IFN-γ (pCMV-Muβ and pCMV-Muγ, respectively) has been shown to be effective in inhibiting the growth of colon carcinoma CT-26 cells in the liver (Kobayashi *et al.*, Molecular Therapy 2002;6:737–44). The therapeutic effect of such IFN gene transfer could be significantly increased by the sustained expression of IFNs. In the present study, CpG-reduced pDNA encoding IFN-β or IFN-γ (pGZB-Muβ and pGZB-Muγ, respectively) was constructed. pCMV-Muβ and pCMV-Muγ were used as conventional CpG-replete pDNAs. Each pDNA was injected into the tail vein of mice by the hydrodynamics-based procedure. An injection of pGZB-Muβ resulted in very high IFN-β activities in the serum for at least 24 hr after injection, whereas the IFN-β activity after pCMV-Muβ injection declined quickly. About a 14-fold greater amount of IFN-β was produced from pGZB-Muβ than from pCMV-Muβ. pGZB-Muβ markedly inhibited the pulmonary metastasis of CT-26 cells. Similar, but more marked results were obtained with pGZB-Muγ: it increased the area under the concentration-time curve by more than a 60-fold and the mean residence time of IFN-γ 4-fold compared with pCMV-Muγ. The survival time of the pGZB-Muγ-treated mice was significantly ($p < 0.05$) longer than that of the saline- or pCMV-Muγ-treated mice. These results indicate that long-term expression of IFN can be achieved by CpG-reduced pDNA and sustained IFN gene expression results in enhanced therapeutic effects of IFN gene transfer against tumor metastasis.**


**Key words:** interferon; cancer gene therapy; pulmonary metastasis; hydrodynamics; CpG dinucleotides

High and sustained transgene expression is indispensable for effective gene therapy. Generally speaking, persistent gene expression increases the therapeutic benefits of gene transfer and reduces the need for redosing. Although plasmid DNA (pDNA), the most frequently-used nonviral vector, avoids the fatal disadvantages that have been experienced with viral vectors, such as virus-induced acute organ failure and insertional mutagenesis, its transgene expression characteristics need to be improved for effective *in vivo* gene therapy.[1,2] The low level of transgene expression has been unacceptable in pDNA-based nonviral vectors for many years, but the development of highly effective nonviral gene delivery methods has now almost solved the problem. The application of electric pulses or ultrasound can significantly increase the level of transgene expression up to 100-fold or more in various experimental settings. In addition Liu *et al.*[3] and Zhang *et al.*[4] have demonstrated that a very high level of transgene expression can be obtained by an intravenous injection of naked pDNA dissolved in a large volume of saline when injected at a high velocity: the so-called hydrodynamics-based procedure.[3] This method of gene delivery results in a high level of transgene expression in internal organs, particularly the liver, apparently unaccompanied by any severe toxicity.[5,6] Therefore, this method could be applied therapeutically with some modifications.[7] However, the transient nature of transgene expression by nonviral vectors is still a major problem associated with nonviral vector-based gene transfer.

Cytokine-supported tumor immunotherapy is a promising strategy for cancer gene therapy. Interferon (IFN) gene transfer is considered to be useful for immunotherapy because IFNs have antiproliferative and immunomodulatory activities which are capable of contributing to the host's defense against tumors.[8–11] We have reported that IFN-β or IFN-γ gene delivery by the hydrodynamics-based procedure is effective in inhibiting the growth of hepatic metastasis of mouse colon carcinoma CT-26 cells.[12] However, we also found that the IFN gene transfer by this procedure was only marginally effective against pulmonary metastasis of the tumor cells. This was associated with the transient concentration of the IFNs in the lung tissue as well as in plasma after the injection of the conventional pDNA encoding IFN-β or IFN-γ.

Systemic administration of a pDNA/cationic liposome complex, or lipoplex, induces several inflammatory cytokines, hematologic changes, and increases the plasma levels of liver enzymes and acute-phase response proteins.[13,14] Such responses can be used as stimuli for transiently increasing pDNA-based transgene expression through the activation of nuclear factor κB.[15] In addition, the nonspecific induction of inflammatory cytokines would be beneficial for cancer gene therapy. However, inflammatory cytokines are reported to reduce the transgene expression at a later time after gene transfer.[16] Early studies have demonstrated that unmethylated CpG dinucleotides in pDNA play significant roles in the induction of inflammatory cytokines through the Toll-like receptor (TLR)-9 upon administration of lipoplex.[17] The cytosine residue of unmethylated CpG dinucleotides in pDNA can also be a target for methylation by DNA methyltransferases.[18,19] Methylated CpG dinucleotides, in turn, recruit the methyl-CpG binding proteins such as MBD1 and MeCP2, which mediate transcriptional repression of the transgene.[20,21] Therefore, the presence of CpG dinucleotides in pDNA may have two adverse consequences: the generation of an inflammatory cytokine response through TLR-9 and the chronic suppression of transgene expression induced by the methylation of CpG dinucleotides as well as by the binding of methyl-CpG binding proteins.

Several approaches have been reported to reduce the number of CpG dinucleotides in pDNA, including the use of polymerase chain reaction (PCR) fragments of pDNA,[22] methylation of the cysteine in CpG dinucleotides by methylase,[23] and the elimination of the sequences.[24] Yew *et al.*[25–27] have reported that a

*Abbreviations:* AUC, area under the plasma concentration-time curve; $C_{max}$, peak plasma concentration; FCS, fetal calf serum; HBSS, Hanks' balanced salt solution; IFN, interferon; MRT, mean residence time; PCR, polymerase chain reaction; pDNA, plasmid DNA; TLR, Toll-like receptor.

Grant sponsors: the Ministry of Education, Culture, Sports, Science and Technology, Japan; the Ministry of Health, Labour and Welfare, Japan; the Uehara Memorial Foundation; the Sankyo Foundation of Life Science.

***Correspondence to:** Department of Biopharmaceutics and Drug Metabolism, Graduate School of Pharmaceutical Sciences, Kyoto University, Sakyo-ku, Kyoto 606-8501, Japan. Fax: +81-75-753-4614.
E-mail: takakura@pharm.kyoto-u.ac.jp

Received 25 August 2006; Accepted after revision 9 January 2007
DOI 10.1002/ijc.22636
Published online 19 March 2007 in Wiley InterScience (www.interscience.wiley.com).

CpG-reduced pDNA, pGZB, in which about 80% of the CpG sequences were depleted from the original vector, showed sustained and enhanced transgene expression after administration to mice in several formulations, such as the naked pDNA and lipoplex. Therefore, the use of the CpG-reduced pDNA may improve the efficacy of IFN gene therapy in various tumor models. In the present study, we inserted murine IFN-β or IFN-γ cDNA into the pGZB vector and examined first whether the expression of the IFNs could be improved by the vector. The expression of the IFNs was quantitatively evaluated using a moment analysis method and the parameters obtained, such as the area under the plasma concentration-time curve (AUC) and mean retention time (MRT), were compared with those obtained after injection of a conventional CpG-replete vector. Then, we examined the therapeutic efficacy of pGZB-based IFN gene delivery by the hydrodynamics-based procedure against the lung metastasis produced by CT-26 cells in mice.

## Material and methods

### *Cell cultures and mice*

A mouse colon carcinoma cell line, CT-26, was cultured in RPMI1640 supplemented with 10% fetal calf serum (FCS). L cells were cultured in 2 g/l glucose-containing Eagle's minimal essential medium supplemented with 6% FCS. Seven-week-old BALB/c mice, purchased from Shizuoka agricultural cooperative association for laboratory animals (Shizuoka, Japan), were maintained under conventional housing conditions. All animal experiments were conducted in accordance with the principles and procedures outlined in the US National Institutes of health guide for the care and use of laboratory animals. The protocols for animal experiments were approved by the Animal Experimentation Committee of Graduate School of Pharmaceutical Sciences, Kyoto University.

### *Plasmid DNA*

pCMV-Luc, pCMV-Muβ and pCMV-Muγ, which were constructed as previously reported,[28,29] were used as CpG-replete pDNA encoding firefly luciferase, mouse IFN-β and mouse IFN-γ, respectively. pGZB vector,[24–27] a CpG-reduced pDNA that has a backbone different from pCMV vectors, was kindly provided by Dr. Yew (Genzyme Corporation, MA, USA). A fragment of mouse *IFN*-β cDNA was amplified by PCR from pCMV-Muβ, and inserted into the *Sfi*I/*Eco*RI site of the pGZB vector to construct pGZB-Muβ. pGZB-Muγ and pGZB-Luc were also constructed in a similar manner. Each pDNA was injected into the tail vein of mice at the indicated doses dissolved in 1.6 ml saline by the hydrodynamics-based procedure.[3,6] The dose of each pDNA was optimized by preliminary experiments; it was set at 10 μg/mouse for IFN-β-expressing pDNA, which was the same dose as in the previous study.[12] Because the injection of pGZB-Muγ at this high dose was found to be lethal to mice, 3 μg was used for IFN-γ-expressing pDNA.

### *Measurement of TNF-α concentration*

The levels of TNF-α in serum were measured using an ELISA kit (AN'ALYZA™, Genzyme, Cambridge, MA) as reported previously.[15] In brief, mice received an intravenous injection of naked pCMV-Luc or pGZB-Luc at a dose of 25 μg/mouse by the hydrodynamics-based procedure. At 1.5 hr after injection, blood was collected from the vena cava of mice under anesthesia, and allowed to stand for 3 hr at 4°C. Then the samples were centrifuged at 3,000*g* for 30 min at 4°C and the serum obtained was used for the assay.

### *Measurement of IFN activity*

To measure the IFN activity in mouse serum, 50–70 μl blood was collected from the tail vein at indicated times after pDNA injection. The blood samples were kept at 4°C for 2–3 hr to allow clotting and then centrifuged to obtain serum. The antiviral activity of IFN-β in the serum was measured using the cytopathic effect of vesicular stomatitis virus on L cells and expressed in international units (IU) as calibrated against the international reference mouse IFN-α, β preparation (NIH-G002-904-511).[30] The concentration of IFN-γ in the serum was determined by ELISA using a commercial kit (Ready-SET-Go! Mouse IFN-γ ELISA, eBioscience). The peak plasma concentrations ($C_{max}$) of IFNs were obtained from the actual data recorded after gene transfer. The AUC and MRT were calculated by integration to infinite time.[31] The normal distribution test was performed using the following equation.[32]

$$Z_0 = \frac{\left|\overline{\phi}_1 - \overline{\phi}_2\right|}{\sqrt{SE_1{}^2 + SE_2{}^2}}$$

where $\overline{\phi}_1$ and $\overline{\phi}_2$ are the means of pharmacokinetic parameters, and $SE_1$ and $SE_2$ are the variances in groups 1 and 2, respectively. If $Z_0 > 1.96$ (confidence interval $p < 0.05$), the difference was assumed to be significant between groups 1 and 2.

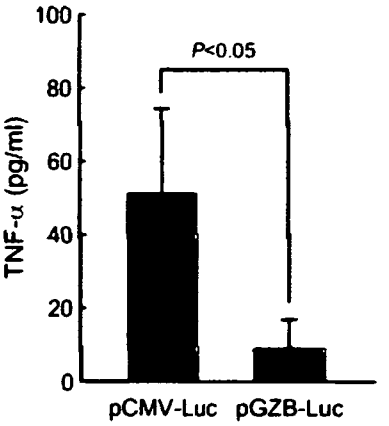


FIGURE 1 – TNF-α level in serum after intravenous injection of pCMV-Luc or pGZB-Luc at a dose of 25 μg/mouse by the hydrodynamics-based procedure. At 1.5 hr after injection, mice were euthanized and blood was collected. Serum concentrations of TNF-α were determined by ELISA. The results are expressed as the mean ± S.D. of 3 mice.

### *Experimental pulmonary metastasis*

CT-26 cells were trypsinized and suspended in Hanks' balanced salt solution (HBSS). The cell suspensions were injected intravenously into syngeneic BALB/c mice at a dose of $1 \times 10^5$ cells in 200 μl HBSS/mouse to establish pulmonary metastasis. Mice inoculated with CT-26 cells were injected intravenously with pDNA by the hydrodynamics-based procedure at indicated times. At 14 days after inoculation of the tumor cells, the lung was excised and the number of pulmonary colonies was counted. In addition, the survival of mice was also evaluated in different animals.

### *Statistical analysis*

Data on the number of metastatic colonies were analyzed by one-way ANOVA followed by the Student-Newmann-Keuls multiple comparison test. Survival of mice was analyzed by a Kaplan-Meier survival plot followed by a log-rank (Mantel-Cox) test.

## Results

### *TNF-α production after injection of pCMV-Luc and pGZB-Luc*

Figure 1 shows the TNF-α concentration in mouse serum 1.5 hr after intravenous injection of pCMV-Luc or pGZB-Luc at a dose of 25 μg/mouse by the hydrodynamics-based procedure. Previous studies indicated that the TNF-α concentration in serum has a

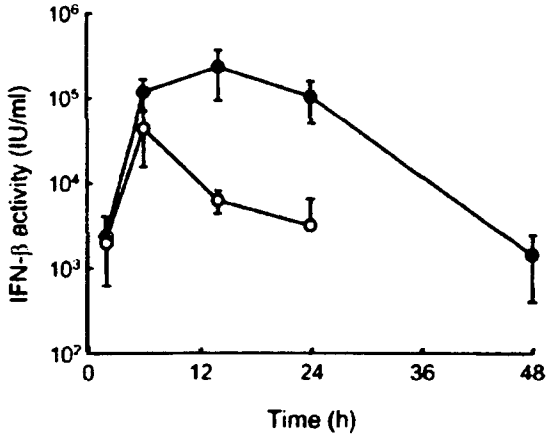


FIGURE 2 – Time-course of the activity of IFN-β in the serum after intravenous injection of pCMV-Muβ (○) or pGZB-Muβ (●) at a dose of 10 μg/mouse by the hydrodynamics-based procedure. The IFN-β activity was measured by bioassay. The activity at 48 hr after injection of pCMV-Muβ was below 400 IU/ml, which is not shown in the figure. The results are expressed as the mean ± SD of 3 mice.

TABLE I – $C_{MAX}$, AUC AND MRT OF SERUM IFN-β AFTER INTRAVENOUS INJECTION OF PCMV-MUβ AND PGZB-MUβ INTO MICE BY THE HYDRODYNAMICS-BASED PROCEDURE

| pDNA | $C_{max}$ (IU/ml) | AUC (IU hr/μl) | MRT (hr) |
|---|---|---|---|
| pCMV-Muβ | 43,000 ± 27,800 | 334 ± 126 | 8.1 ± 2.6 |
| pGZB-Muβ | 227,000 ± 134,000 | 4,520 ± 650* | 16.7 ± 3.6* |

The $C_{max}$ values were determined at 6 and 14 h after intravenous injection of pCMV-Muβ and pGZB-Muβ, respectively, by the hydrodynamics-based procedure at a dose of 10 μg/mouse, and are expressed as the mean ± SD of three mice. The AUC and MRT were calculated by integration to infinite time, and are expressed as the calculated mean ± SE.

*Statistically significant ($p < 0.05$) compared with pCMV-Muβ.

peak value around 1.5 hr after injection of various pDNA formulations. The injection of the CpG-replete pCMV-Luc resulted in the peak TNF-α concentration of 51 ± 23 pg/ml, which was significantly greater than that of pGZB-Luc (8.9 ± 8.0 pg/ml). However, these levels of TNF-α production were much lower than those obtained with pDNA/cationic liposome complexes, some of which resulted in a peak TNF-α concentration of 500 pg/ml or greater at the same dose of pDNA.[12,15]

*IFN-β activity after injection of pCMV-Muβ and pGZB-Muβ*

Figure 2 shows the time-courses of the IFN-β concentrations in serum after intravenous injection of pCMV-Muβ or pGZB-Muβ at a dose of 10 μg/mouse. High IFN-β activities were detected after injection of pCMV-Muβ by the hydrodynamics-based procedure with a peak level of 43,000 ± 27,800 IU/ml at 6 hr after injection. However, the activity declined quickly with time and was below 400 IU/ml by 48 hr. In contrast, the IFN-β activities after injection of pGZB-Muβ were significantly greater than those of pCMV-Muβ at any sampling point except for 2 hr. About a 5-fold greater peak level (227,000 ± 134,000 IU/ml) was obtained at 14 hr after injection, and a significant level of activity could be detected at 48 hr after injection. Table I summarizes the pharmacokinetic parameters of serum IFN-β after injection of each IFN-β-expressing pDNA. The AUC values were calculated to be 334 ± 126 and 4,520 ± 650 IU hr/l after injection of pCMV-Muβ and pGZB-Muβ ($p < 0.05$), respectively, indicating that about a 14-fold greater amount of IFN-β was produced from pGZB-Muβ than from pCMV-Muβ. A long MRT (16.7 ± 3.6 hr) was obtained with pGZB-Muβ, which was statistically ($p < 0.05$) significantly different from that of pCMV-Muβ (8.1 ± 2.6 hr).

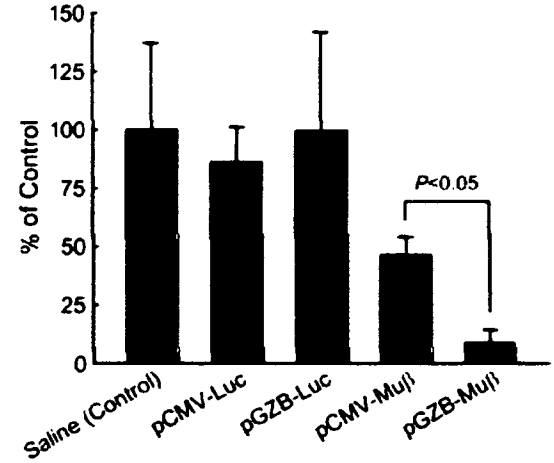


FIGURE 3 – Effect of IFN-β gene transfer on the pulmonary metastasis of CT-26 cells in mice. Mice were inoculated with CT-26 cells by a tail vein injection at a dose of $1 \times 10^5$ cells/mouse (day 0). At 24 hr after inoculation, mice were injected intravenously with saline (control), pCMV-Luc, pGZB-Luc, pCMV-Muβ or pGZB-Muβ at a dose of 10 μg/mouse by the hydrodynamics-based procedure. On day 14, mice were euthanized and the number of metastatic colonies on the lung surface was counted. The results are normalized to the control value (226 ± 84, the saline-treated group) and are expressed as the mean ± SD of at least 4 mice.

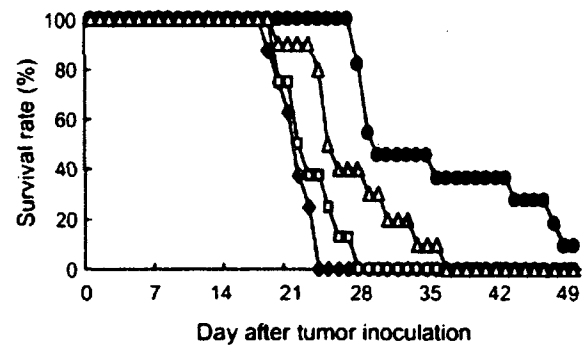


FIGURE 4 – Effect of IFN-β gene transfer on the survival rate of mice bearing pulmonary metastasis of CT-26 cells. Mice inoculated with $1 \times 10^5$ CT-26 cells were treated with saline (control, ◆), pCMV-Luc (□), pCMV-Muβ (△) or pGZB-Muβ (●) at a dose of 10 μg/mouse by the hydrodynamics-based procedure at 24 hr after tumor inoculation. Each group consisted of at least 9 mice.

*Effects of IFN-β-expressing pDNA on pulmonary metastasis in mice*

Inoculation of CT-26 cells into the tail vein of mice resulted in the formation of 226 ± 84 metastatic colonies on the lung surface at 14 days (Fig. 3). pCMV-Muβ or pGZB-Muβ (10 μg/mouse) significantly reduced the number of metastatic colonies following a single injection at 24 hr after the inoculation of CT-26 cells: 46.3% ± 7.9% and 8.6% ± 5.6% of the colonies were found in pCMV-Muβ-treated and pGZB-Muβ-treated mice, respectively, compared with the number in the saline-treated controls. pCMV-Luc (86.0% ± 15.1%) or pGZB-Luc (99.3% ± 42.5%) had little effect on the number of metastatic colonies in mouse lung at the same dose (10 μg), suggesting that the reduction in the number of metastatic colonies is mediated by IFN-β activity.

Figure 4 shows the survival rate of CT-26-bearing mice receiving a single injection of each pDNA (10 μg/mouse). The pCMV-Muβ- or pGZB-Muβ-treated mice survived significantly ($p < 0.05$) longer than the pCMV-Luc-treated mice. The mean survival

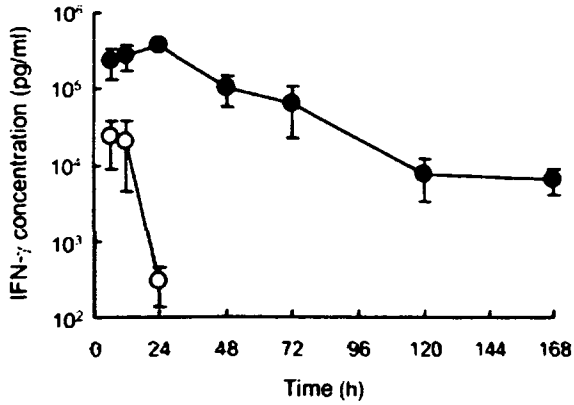


FIGURE 5 – Time-course of the concentration of IFN-γ in serum after intravenous injection of pCMV-Muγ (○) or pGZB-Muγ (●) at a dose of 3 μg/mouse by the hydrodynamics-based procedure. The IFN-γ concentration was measured by ELISA. The concentrations at 36 hr or later after injection of pCMV-Muγ were below the detection limit of 15 pg/ml. The results are expressed as the mean ± SD of at least 3 mice.

TABLE II – $C_{MAX}$, AUC AND MRT OF SERUM IFN-γ AFTER INTRAVENOUS INJECTION OF PCMV-MUγ AND PGZB-MUγ INTO MICE BY THE HYDRODYNAMICS-BASED PROCEDURE

| pDNA | $C_{max}$ (pg/ml) | AUC (pg hr/μl) | MRT (hr) |
|---|---|---|---|
| pCMV-Muγ | 23,300 ± 14,700 | 262 ± 38 | 8.9 ± 1.8 |
| pGZB-Muγ | 382,000 ± 50,600* | 15,900 ± 900* | 34.8 ± 3.7* |

The $C_{max}$ values were obtained at 6 hr and 24 hr after intravenous injection of pCMV-Muβ and pGZB-Muβ, respectively, by the hydrodynamics-based procedure at a dose of 3 μg/mouse, and are expressed as the mean ± SD of at least three mice. The AUC and MRT were calculated by integration to infinite time, and are expressed as the calculated mean ± SE.

*Statistically significant ($p < 0.05$) compared with pCMV-Muγ.

times of mice treated with pCMV-Luc, pCMV-Muβ and pGZB-Muβ were 20.8 ± 1.5, 22.8 ± 3.1 and 26.6 ± 5.1 days, respectively. No statistically significant difference was obtained between the pCMV-Muβ and pGZB-Muβ-treated groups as far as the survival of CT-26-bearing mice was concerned.

*IFN-γ concentration after injection of pCMV-Muγ and pGZB-Muγ*

Figure 5 shows the time-courses of the IFN-γ concentration in serum after intravenous injection of pCMV-Muγ or pGZB-Muγ at a dose of 3 μg/mouse. Again, sustained IFN-γ concentrations were observed in mice receiving CpG-reduced pGZB-Muγ. More than 10,000 pg IFN-γ/ml was detected in the serum from 6 hr to 3 days after injection of pGZB-Muγ, whereas the concentrations were below the detection limit at 36 hr or later after injection of pCMV-Muγ. The initial IFN-γ concentration after injection of pGZB-Muγ was much greater than that after pCMV-Muγ ($p < 0.05$). In addition, the IFN concentration declined with a longer half-life in mice receiving pGZB-Muγ than in those receiving pCMV-Muγ, suggesting prolonged expression of IFN-γ by pGZB-Muγ. These expression properties of both vectors resulted in significant differences ($p < 0.05$) in the pharmacokinetic parameters (Table II): more than a 60-fold greater AUC and an about 4-fold longer MRT were obtained when pGZB-Muγ was injected in place of pCMV-Muγ.

*Effects of IFN-γ-expressing pDNA on pulmonary metastasis in mice*

Mice receiving CT-26 cells by intravenous injection were injected intravenously with pGZB-Muγ, pCMV-Muγ, pGZB-Luc or pCMV-Luc (3 μg/mouse) by the hydrodynamics-based procedure at 1 day after tumor inoculation. Figure 6 shows the number of metastatic colonies on the lung surface measured at 14 days

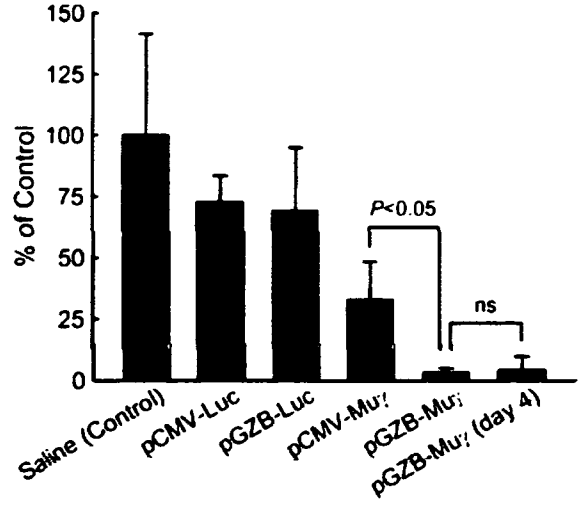


FIGURE 6 – Effect of IFN-γ gene transfer on the pulmonary metastasis of CT-26 cells in mice. Mice were inoculated with CT-26 cells by a tail vein injection at a dose of $1 \times 10^5$ cells/mouse (day 0). At 24 hr after inoculation, mice were injected intravenously with saline (control), pCMV-Luc, pGZB-Luc, pCMV-Muγ or pGZB-Muγ at a dose of 3 μg/mouse by the hydrodynamics-based procedure. On day 14, mice were euthanized and the number of metastatic colonies on the lung surface was counted. The results are normalized to the control value (215 ± 89, the saline-treated group) and are expressed as the mean ± SD of at least 4 mice.

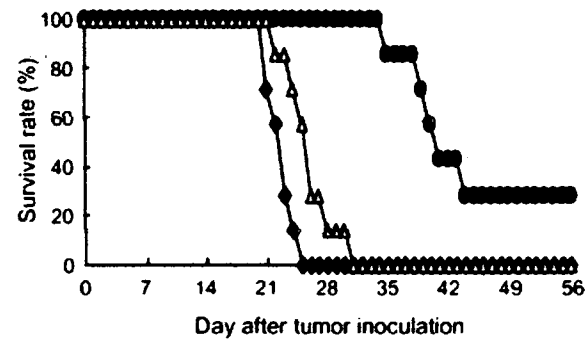


FIGURE 7 – Effect of IFN-γ gene transfer on the survival rate of mice bearing pulmonary metastasis of CT-26 cells. Mice inoculated with $1 \times 10^5$ CT-26 cells were treated with saline (control, ◆), pCMV-Muγ (△) or pGZB-Muγ (●) at a dose of 3 μg/mouse by the hydrodynamics-based procedure at day 1, 14, and 28 after tumor inoculation. Each group consisted of at least 7 mice.

after inoculation. pCMV-Muγ and pGZB-Muγ reduced the number of colonies to 32.8% ± 15.7% and 3.4% ± 1.7% of those in the saline-treated group (215 ± 89 colonies). To examine the effect of the interval of tumor inoculation and IFN-γ gene transfer, pGZB-Muγ was injected 4 days after tumor inoculation. This treatment also reduced the number of colonies to 4.4% ± 5.5% of those in the saline-treated group, which was not significantly different from the pGZB-Muγ-treated group injected 1 day after tumor inoculation. No significant reduction was obtained by pCMV-Luc (72.7% ± 10.7%) or pGZB-Luc (69.1% ± 25.9 %). Then, the survival of CT-26-bearing mice was examined in different sets of mice, which received 3 injections of pCMV-Muγ or pGZB-Muγ (3 μg/mouse/shot) at day 1, 14 and 28 after tumor inoculation (Fig. 7). The mean survival times of the saline-treated group and the pCMV-Muγ-treated group were 21.7 ± 1.5 and 25.0 ± 2.9 days, respectively, and the difference was not statistically significant. In contrast, the survival time of the pGZB-Muγ-treated mice

was significantly ($p < 0.05$) longer than that of the other groups. Furthermore, 2 out of 7 mice survived more than 56 days.

## Discussion

We have already reported that IFN-β or IFN-γ gene delivery by the hydrodynamics-based procedure results in a significant antitumor effect against hepatic metastasis, but a weaker effect against pulmonary metastasis, of mouse colon carcinoma CT-26 cells.[12] The hydrodynamics-based procedure results in transgene expression in various internal organs, but the expression in the lung is much lower than that in the liver.[3] In a previous study, we could detect high IFN activities in the liver after gene transfer by this procedure, but failed to detect significant concentrations of IFNs in the lung. In addition, the plasma concentration of IFNs after gene transfer declined very quickly because of the transient nature of the gene expression driven by the conventional CMV promoter. These characteristics of the hydrodynamic delivery of IFN genes using conventional pDNA with CMV promoter explain the low efficacy of IFN gene transfer against pulmonary metastasis in mice. Consequently, to increase the therapeutic efficacy of IFN cancer gene therapy, we tried to increase and prolong the IFN expression by reducing CpG dinucleotides in pDNA.

As reported with other reporter and therapeutic genes,[25–27,33] the expression of IFN-β and IFN-γ from the pGZB vectors, which was estimated from their serum concentration profiles, was much longer than that from conventional pDNA after intravenous injection by the hydrodynamics-based procedure. A similar prolonged expression with pGZB vector was also obtained with firefly *luciferase* gene (unpublished data). Early studies have claimed that inflammatory cytokines, such as TNF-α produced after pDNA administration, reduce the transgene expression. In the present study, we found that the serum TNF-α level was significantly lower in mice receiving pGZB-Luc than in mice receiving pCMV-Luc (Fig. 1), suggesting that a reduced production of inflammatory cytokines is involved in the prolonged expression of IFNs from the pGZB vector. However, the low and transient nature of the induction of inflammatory cytokines after the injection of naked pDNA by the hydrodynamics-based procedure suggests that sustained gene expression from the pGZB vector is due not only to a reduction of the inflammatory response, but also to other mechanisms that have so far not been investigated.[33]

Transcriptional repression of endogenous genes is often associated with a higher frequency of methylated cytosine residues in the 5′ flanking region of the genes: promoter or enhancer.[34,35] Moreover, CpG methylation has been reported to be associated with the absence of integrated viral gene expression[36] and it has been suggested that *de novo* methylation of foreign DNA represents a cellular defense mechanism against the transcription of a foreign gene.[37] Because all CpG dinucleotides, except for those in the replication origin region, were converted to TpG dinucleotides in the pGZB vector, there was no substrate for DNA methyltransferase in the regions that were relevant to transgene expression. Therefore, sustained gene expression from CpG-reduced pDNA might be closely related to CpG methylation in addition to the reduced inflammatory response.

It has already been reported that the expression of reporter genes, such as chloramphenicol acetyltransferase or a secreted form of human placental alkaline phosphatase, is prolonged by the removal of CpG dinucleotides from the vectors.[25–27] In the present study, we also obtained a sustained transgene expression of either mouse IFN-β or IFN-γ by using CpG-reduced pDNA. However, the expression of IFN-β was not as persistent as that of IFN-γ and other proteins in the literature, suggesting that some of the pharmacological activities of IFN-β shut off the expression. Recently, Sellins *et al.*[38] reported that type I IFNs, such as IFN-α and IFN-β, play a key role in suppressing transgene expression following systemic *in vivo* gene transfer. To examine the effects of IFN-β as well as IFN-γ on transgene expression, the transgene expression in the liver was examined in mice using the pDNA encoding firefly *luciferase* gene (pGZB-Luc). Preadministration of pGZB-Muβ or pGZB-Muγ 48 hr prior to the hydrodynamic delivery of pGZB-Luc reduced the luciferase activity in the liver, but the reduction was significantly greater with pGZB-Muβ (data not shown). Therefore, it is probable that a moderate persistence of IFN-β activity after injection of pGZB-Muβ is a consequence of the ability of IFN-β to affect transcription of the transgene.

The increase in the IFN-β activity, which was quantitatively evaluated by a pharmacokinetic analysis to be a 14-fold increase in the AUC, led to a drastic reduction in the number of metastatic colonies in the lung. However, there was no significant difference in the survival time of the tumor-bearing mice between pCMV-Muβ-treated and pGZB-Muβ-treated groups. On the other hand, the use of pGZB-Muγ produced a significantly greater increase in the AUC (60-fold) and MRT (4-fold), resulting in a significant reduction in the number of tumor colonies as well as a significant increase in the survival time. Taken together, these results demonstrate that long-term expression of either IFN can be achieved by CpG-reduced pDNA and that sustained IFN gene expression results in enhanced therapeutic effects against lung metastasis of tumor cells. IFN-γ gene transfer was much more effective in increasing the survival of CT-26-bearing mice than IFN-β gene transfer, probably reflecting the greater increase in the serum IFN concentrations following the use of pGZB vector. Although multiple injections of conventional pDNA, such as pCMV-Muγ, could be effective in increasing the anti-cancer effect of IFNs, high and sustained serum concentrations of IFN-γ achieved by the pGZB-Muγ will not be obtained by increasing the frequency of administration of pCMV-Muγ. However, too high levels of IFN could induce toxic effects as observed in mice receiving 10 μg of pGZB-Muγ (data not shown). Therefore, the administration dose of pDNA should be carefully adjusted for future clinical applications.

Transfection of CT-26 cells with the IFN genes may occur by the hydrodynamic delivery of pDNA, which could be responsible for the antitumor effects of IFN gene transfer as reported in previous studies.[39,40] However, the level of transgene expression in the liver is far greater than those in other organs,[3] including the lung, the organ where metastatic tumor cells colonize in the present study. We also demonstrated a similar organ expression spectrum of the transgene following injection of pCMV-Muβ and pCMV-Muγ.[12] Therefore, direct transfection of tumor cells with the IFN genes, if it occurs, could have little contribution to the antitumor effects of hydrodynamic IFN gene transfer.

In conclusion, the CpG depletion from pDNA has been proved to be a useful approach for IFN cancer gene therapy. Because the sustained expression from pGZB vector may not be specific for its intravenous injection by the hydrodynamics-based procedure, less invasive methods of administration may be possible for future applications of IFN gene transfer to patients.

## Acknowledgements

The authors thank Dr Seng H. Cheng and Dr Nelson S. Yew (Genzyme Corporation) for providing the pGZB vector.

## References

1. Nishikawa M, Huang L. Nonviral vectors in the new millennium: delivery barriers in gene transfer. Hum Gene Ther 2001;12:861–70.
2. Nishikawa M, Hashida M. Nonviral approaches satisfying various requirements for effective in vivo gene therapy. Biol Pharm Bull 2002;25:275–83.
3. Liu F, Song Y, Liu D. Hydrodynamics-based transfection in animals by systemic administration of plasmid DNA. Gene Ther 1999;6:1258–66.
4. Zhang G, Budker V, Wolff JA. High levels of foreign gene expression in hepatocytes after tail vein injections of naked plasmid DNA. Hum Gene Ther 1999;10:1735–7.

5. Song YK, Liu F, Zhang G, Liu D. Hydrodynamics-based transfection: simple and efficient method for introducing and expressing transgenes in animals by intravenous injection of DNA. Methods Enzymol 2002;346:92–105.
6. Kobayashi N, Nishikawa M, Takakura Y. The hydrodynamics-based procedure for controlling the pharmacokinetics of gene medicines at whole body, organ and cellular levels. Adv Drug Deliv Rev 2005; 57:713–31.
7. Eastman SJ, Baskin KM, Hodges BL, Chu Q, Gates A, Dreusicke R, Anderson S, Scheule RK. Development of catheter-based procedures for transducing the isolated rabbit liver with plasmid DNA. Hum Gene Ther 2002;13:2065–77.
8. Gansbacher B, Bannerji R, Daniels B, Zier K, Cronin K, Gilboa E. Retroviral vector-mediated γ-interferon gene transfer into tumor cells generates potent and long lasting antitumor immunity. Cancer Res 1990;50:7820–5.
9. Yanagihara K, Seyama T, Watanabe Y. Antitumor potential of interferon-γ: retroviral expression of mouse interferon-γ cDNA in two kinds of highly metastatic mouse tumor lines reduces their tumorigenicity. Nat Immun 1994;13:102–12.
10. Singh RK, Gutman M, Bucana CD, Sanchez R, Llansa N, Fidler IJ. Interferons α and β down-regulate the expression of basic fibroblast growth factor in human carcinomas. Proc Natl Acad Sci USA 1995;92:4562–6.
11. Albini A, Marchisone C, Del Grosso F, Benelli R, Masiello L, Tacchetti C, Bono M, Ferrantini M, Rozera C, Truini M, Belardelli F, Santi L et al. Inhibition of angiogenesis and vascular tumor growth by interferon-producing cells: a gene therapy approach. Am J Pathol 2000;156:1381–93.
12. Kobayashi N, Kuramoto T, Chen S, Watanabe Y, Takakura Y. Therapeutic effect of intravenous interferon gene delivery with naked plasmid DNA in murine metastasis models. Mol Ther 2002;6:737–44.
13. Li S, Wu SP, Whitmore M, Loeffert EJ, Wang L, Watkins SC, Pitt BR, Huang L. Effect of immune response on gene transfer to the lung via systemic administration of cationic lipidic vectors. Am J Physiol 1999;276:L796–L804.
14. Whitmore M, Li S, Huang L. LPD lipopolyplex initiates a potem cytokine response and inhibits tumor growth. Gene Ther 1999;6: 1867–75.
15. Kuramoto T, Nishikawa M, Thanaketpaisarn O, Okabe T, Yamashita F, Hashida M. Use of lipoplex-induced nuclear factor-κB activation to enhance transgene expression by lipoplex in mouse lung. J Gene Med 2006;8:53–62.
16. Tan Y, Li S, Pitt BR, Huang L. The inhibitory role of CpG immunostimulatory motifs in cationic lipid vector-mediated transgene expression in vivo. Hum Gene Ther 1999;10:2153–61.
17. Hemmi H, Takeuchi O, Kawai T, Kaisho T, Sato S, Sanjo H, Matsumoto M, Hoshino K, Wagner H, Takeda K, Akira S. A Toll-like receptor recognizes bacterial DNA. Nature 2000;408:740–5.
18. Hsieh CL. In vivo activity of murine de novo methyltransferases, Dnmt3a and Dnmt3b. Mol Cell Biol 1999;19:8211–18.
19. Bestor TH. The DNA methyltransferases of mammals. Hum Mol Genet 2000;9:2395–402.
20. Hendrich B, Bird A. Identification and characterization of a family of mammalian methyl-CpG binding proteins. Mol Cell Biol 1998;18: 6538–47.
21. Fujita N, Shimotake N, Ohki I, Chiba T, Saya H, Shirakawa M, Nakao M. Mechanism of transcriptional regulation by methyl-CpG binding protein MBD1. Mol Cell Biol 2000;20:5107–18.
22. Hofman CR, Dileo JP, Li Z, Li S, Huang L. Efficient in vivo gene transfer by PCR amplified fragment with reduced inflammatory activity. Gene Ther 2001;8:71–4.
23. Reyes-Sandoval A, Ertl HC. CpG methylation of a plasmid vector results in extended transgene product expression by circumventing induction of immune responses. Mol Ther 2004;9:249–61.
24. Yew N, Cheng SH. Reducing the inflammatory activity of CpG-containing plasmid DNA vectors for non-viral gene therapy. Expert Opin Drug Deliv 2004;1:115–25.
25. Yew NS, Wang KX, Przybylska M, Bagley RG, Stedman M, Marshall J, Scheule RK, Cheng SH. Contribution of plasmid DNA to inflammation in the lung after administration of cationic lipid:pDNA complexes. Hum Gene Ther 1999;10:223–34.
26. Yew NS, Zhao H, Wu IH, Song A, Tousignant JD, Przybylska M, Cheng SH. Reduced inflammatory response to plasmid DNA vectors by elimination and inhibition of immunostimulatory CpG motifs. Mol Ther 2000;1:255–62.
27. Yew NS, Zhao H, Przybylska M, Wu IH, Tousignant JD, Scheule RK, Cheng SH. CpG-depleted plasmid DNA vectors with enhanced safety and long-term gene expression in vivo. Mol Ther 2002;5:731–8.
28. Kawabata K, Takakura Y, Hashida M. The fate of plasmid DNA after intravenous injection in mice: involvement of scavenger receptors in its hepatic uptake. Pharm Res 1995;12:825–30.
29. Nomura T, Yasuda K, Yamada T, Okamoto S, Mahato RI, Watanabe Y, Takakura Y, Hashida M. Gene expression and antitumor effects following direct interferon (IFN)-γ gene transfer with naked plasmid DNA and DC-chol liposome complexes in mice. Gene Ther 1999;6:121–9.
30. Watanabe Y, Kawade Y. Induction, production, and purification of natural mouse IFN-α and -β. In: Clemens MJ, Morris AG, Gearing AJH, eds. Lymphokines and interferons: A practical approach. Oxford: IRL Press, 1987. p. 1–14.
31. Yamaoka K, Nakagawa T, Uno T. Statistical moments in pharmacokinetics. J Pharmacokinet Biopharm 1978;6:547–58.
32. Bailer AJ. Testing for the equality of area under the curves when using destructive measurement techniques. J Pharmacokinet Biopharm 1988;16:303–9.
33. Hodges BL, Taylor KM, Joseph MF, Bourgeois SA, Scheule RK. Long-term transgene expression from plasmid DNA gene therapy vectors is negatively affected by CpG dinucleotides. Mol Ther 2004;10:269–78.
34. Robertson KD, Wolffe AP. DNA methylation in health and disease. Nat Rev Genet 2000;1:11–9.
35. Ballestar E, Wolffe AP. Methyl-CpG-binding proteins. Targeting specific gene repression. Eur J Biochem 2001;268:1–6.
36. Sutter D, Doerfler W. Methylation of integrated adenovirus type 12 DNA sequences in transformed cells is inversely correlated with viral gene expression. Proc Natl Acad Sci USA 1980;77:253–6.
37. Doerfler W. DNA methylation: eukaryotic defense against the transcription of foreign genes? Microb Pathog 1992;12:1–8.
38. Sellins K, Fradkin L, Liggitt D, Dow S. Type I interferons potently suppress gene expression following gene delivery using liposome-DNA complexes. Mol Ther 2005;12:451–9.
39. Esumi N, Hunt B, Itaya T, Frost P. Reduced tumorigenicity of murine tumor cells secreting gamma-interferon is due to nonspecific host responses and is unrelated to class I major histocompatibility complex expression. Cancer Res 1991;51:1185–9.
40. Xie K, Bielenberg D, Huang S, Xu L, Salas T, Juang SH, Dong Z, Fidler IJ. Abrogation of tumorigenicity and metastasis of murine and human tumor cells by transfection with the murine IFN-β gene: possible role of nitric oxide. Clin Cancer Res 1997;3:2283–94.

# DNA and its cationic lipid complexes induce CpG motif-dependent activation of murine dendritic cells

Takaharu Yoshinaga, Kei Yasuda, Yoshiyuki Ogawa, Makiya Nishikawa and Yoshinobu Takakura

*Department of Biopharmaceutics and Drug Metabolism, Graduate School of Pharmaceutical Sciences, Kyoto University, Kyoto, Japan*

doi:10.1111/j.1365-2567.2006.02451.x
Received 13 March 2006; revised 5 July 2006; accepted 5 July 2006.
Correspondence: Dr Y. Takakura, Department of Biopharmaceutics and Drug Metabolism, Graduate School of Pharmaceutical Sciences, Kyoto University, 46-29, Yoshidashimoadachi-cho, Sakyo-ku, Kyoto 606-8501, Japan.
Email: takakura@pharm.kyoto-u.ac.jp
Senior author: Yoshinobu Takakura

## Summary

**Unmethylated CpG motifs in bacterial DNA, but not in vertebrate DNA, are known to trigger an inflammatory response of antigen-presenting cells (APC). In this study, we investigated the cytokine release from murine dendritic cells (DC) by the addition of various types of DNA in the free or complexed form with cationic lipids. Naked plasmid DNA and *Escherichia coli* DNA with immunostimulatory unmethylated CpG motifs induced pro-inflammatory cytokine secretion from granulocyte–macrophage colony-stimulating factor (GM-CSF)-cultured bone marrow-derived DC and the DC cell-line, DC2.4 cells, though vertebrate calf thymus DNA (CT DNA) with less CpG motifs did not. These characteristics differed from mouse peritoneal resident macrophages that do not respond to any naked DNA. The amount of cytokines released from the DC was significantly increased by complex formation with cationic lipids when CpG-motif positive DNAs were used. Unlike murine macrophages or Flt-3 L cultured DC, GM-CSF DC did not release inflammatory cytokines in response to the addition of CT DNA/cationic lipid complex, suggesting that the activation is completely dependent on CpG motifs. Taken together, the results of the present study demonstrate that murine DC produce pro-inflammatory cytokines upon stimulation with CpG-containing DNAs and the responses are enhanced by cationic lipids. These results also suggest that DC are the major cells that respond to naked CpG DNA *in vivo*, although both DC and macrophages will release inflammatory cytokines after the administration of a DNA/cationic lipid complex.**

**Keywords:** CpG motifs; dendritic cells; TLR9; DNA and DNA uptake

## Introduction

It is well known that unmethylated CpG sequences (CpG motifs) in bacterial DNA, but not in vertebrate DNA, are recognized by the immune system as a danger signal.[1] Cytokines such as tumour necrosis factor-α (TNF-α), interleukin-6 (IL-6), IL-12 and interferon-α (IFN-α) are secreted from antigen presenting cells, especially macrophages or dendritic cells (DC), upon stimulation with CpG DNA and synthetic oligodeoxynucleotides (ODN) containing CpG motifs. These cytokines significantly modify the therapeutic effects of DNA-based therapies in different ways.[2] For example, in gene therapy, cytokine production generally seems inappropriate because these inflammatory cytokines significantly reduce transgene expression in target cells through their direct

Abbreviations: APC, antigen-presenting cells; DC, dendritic cells; BMDC, bone-marrow derived dendritic cell; CT DNA, calf thymus DNA; TNF-α, tumour necrosis factor-α; IL-6, interleukin-6; IL-12, interleukin-12; IFN-α, interferon-α; ELISA, enzyme-linked immunosorbent assay; FBS, fetal bovine serum; IRF, interferon regulatory factor; LPS, lipopolysaccharide; ODN, oligodeoxynucleotide; MHC, major histocompatibility complex; TLR, Toll-like receptor; JNK, c-Jun $NH_2$-terminal kinase; Flt-3 L DC, Flt-3ligand cultured bone-marrow dendritic cells; EC DNA, *Escherichia coli* DNA, pDNA, plasmid DNA; FL-pDNA, fluorescein labelled plasmid DNA; GM-CSF, DC; granulocyte–macrophage, colony-stimulating factor cultured dendritic cells; DNase II, deoxyribonuclease II.

 

cytotoxicity and promoter attenuation.[3–5] On the other hand, it is essential for DNA vaccination because these cytokines can enhance the immune responses and profoundly affect the balance of these cytokines and the nature of the immune responses.[6–9]

DC are one of the most important cell populations as far as both innate and acquired immunity are concerned. They influence a variety of immunological responses associated with the therapeutic use of CpG DNA.[10,11] In addition to cytokine secretion, the expression of surface major histocompatibility complex (MHC) class I and II molecules as well as costimulatory molecules increases, and the maturation of DC is induced upon stimulation with CpG motifs.[12] The initial important step for all these processes associated with CpG DNA is cellular uptake because the receptor of CpG DNA, Toll-like receptor-9 (TLR9), is expressed within cells.[13,14] Our previous *in vitro* study using a DC cell line, DC2.4 cells, in mice demonstrated that DC take up pDNA via a mechanism specific to some defined polyanions[15] similar to cultured mouse peritoneal macrophages.[16,17]

There is a rapidly growing body of information about the mechanism of antigen-presenting cell (APC) activation by CpG DNA. This activation requires endosomal acidification and recognition by TLR9.[18–20] CpG DNA appears to use a TLR9 signaling pathway for NF-κB and c-Jun $NH_2$-terminal kinase (JNK) and IRF-7 through MyD88.[19,21] However, these proposed mechanisms are mainly based on studies using synthetic phosphorothioate CpG ODN, and there is little information about the activation induced by native DNA. Our previous study has demonstrated that, in contrast to macrophage cell lines, primary cultured mouse peritoneal macrophages secrete almost no inflammatory cytokines upon stimulation with pDNA, in spite of extensive uptake of the CpG DNA[22]. However, DNA/cationic lipid complex can activate the murine macrophages to induce inflammatory cytokines, whether they have replete CpG motifs or not.[23] Flt-3-ligand cultured bone-marrow DC (Flt-3 L DC) exhibit a different type of activation.[24,25] Upon stimulation with naked DNA, bacterial pDNA and CpG ODN stimulate Flt-3 L DC to induce cytokines IFN-α or IL-6 although vertebrate CT DNA does not. However, TLR9 in Flt-3 L DC can react when CT DNA is combined with cationic lipid N-[1-(2,3-dioleoyloxy)propyl]-N,N,N-trimethylammonium methylsulfate (DOTAP).[24] Methylated CpG motifs or non-canonical CpG motifs complexed with DOTAP induce the activation of TLR9 in Flt-3 L DC. Further experiments have proved that the other sequences also induce the activation of TLR9 when ODNs are translocated to endosomes by DOTAP.[25] While receptor-mediated endocytosis restricts the uptake of DNA, adsorptive endocytosis by cationic lipids does not. Thus, enhancement of DNA uptake seems to control the activation of TLR9 by vertebrate DNA. In the present study, we used a different type of DC and showed that the cells could respond to only DNA with CpG motifs even if the DNA was translocated to endosomes by cationic lipids.

## Materials and methods

### *Chemicals*

RPMI-1640 medium was obtained from Nissui Pharmaceutical (Tokyo, Japan). *Escherichia coli* DNA (EC DNA) and calf thymus DNA (CT DNA) were purchased from Sigma (St Louis, MO). Lipofectin reagent and Opti-MEM were purchased from Invitrogen (Rockville, MD). Mouse recombinant GM-CSF (rGM-CSF) and Triton-X-114 were purchased from Nacalai Tesque (Kyoto, Japan). [α-$^{32}$P]dCTP (3000 Ci/mmol) was obtained from Amersham (Amersham, UK). Fetal Bovine Serum (FBS) was purchased from Thermo Trace (Melbourne, Australia).

### *Cell culture*

Male ICR mice (5 weeks) were purchased from Shizuoka Agricultural Cooperative Association for Laboratory Animals (Shizuoka, Japan). After bone marrow was flushed out of the bones of the hind legs of the mice, the cells were cultured in RPMI-1640 medium supplemented with 10% fetal bovine serum (FBS) and 1000 U/ml rGM-CSF. After a 4–5 day incubation at 37° in 5% $CO_2$-95% air, cells were collected and centrifuged at 200 *g* for 10 min. After removal of the supernatant, the cells were resuspended in 400 μl phosphate-buffered saline (PBS) containing 0·5% bovine serum albumin (BSA) per $10^8$ total cells. The cell suspension was mixed thoroughly with 100 μl magnetic-activated cell sorting (MACS) CD11c MicroBeads (Miltenyi Biotec, Germany), and incubated for 15 min at 4°. After incubation, the cells were washed, centrifuged at 200 *g* for 10 min, and resuspended in 500 μl PBS containing 0·5% BSA. Then, magnetic separation with MACS was carried out to isolate the DC by selecting CD11c-positive cells from the cultured cells. These isolated cells were washed and then plated on 24-well culture plates (Falcon, Becton Dickinson, Lincoln Park, NJ) at a density of $5 \times 10^5$ cells/well and cultured for 24 hr. The murine DC2.4 cells were a gift from Dr Kenneth Rock (Department of Pathology, University of Massachusetts Medical School, MA). DC2.4 cells display dendritic morphology, express dendritic cell-specific markers, MHC molecules, and costimulatory molecules, and exhibit phagocytic activity and an antigen-presenting capacity.[26] DC2.4 cells were cultured with RPMI-1640 medium supplemented with 10% FBS, 2 mM L-glutamine, 100 μM non-essential amino acids, 50 μM 2-mercaptoethanol, and antibiotics. They were then plated on a 24-well culture plate at a density of $5 \times 10^5$ cells/well and cultured for 24 hr.

*DNA*

pCMV-Luc encoding firefly luciferase gene was constructed, as described previously.[27] pDNA was purified using an Endo-free plasmid Giga kit (Qiagen, Valencia, CA). For the cellular association experiments, pDNA was radiolabelled with [α-$^{32}$P]dCTP by nick translation.[28] For the activation experiments, all DNA samples were extensively purified with Triton-X-114, a non-ionic detergent, to minimize the activation by contaminated lipopolysaccharide (LPS). Extraction of endotoxin from pDNA, EC DNA, and CT DNA samples was performed according to reviously published methods[29,30] with slight modifications. DNA samples were purified by extraction with phenol : chloroform : isoamyl alcohol (25 : 24 : 1) and ethanol precipitation. Then, 10 mg DNA was diluted with 20 ml pyrogen-free water, followed by the addition of 200 μl Triton-X-114 and mixing. The solution was placed on ice for 15 min and incubated for 15 min at 55°. Subsequently, the solution was centrifuged for 20 min at 25°, 600 *g*. The upper phase was transferred to a new tube, 200 μl Triton-X-114 was added, and the previous steps were repeated at least three times. The activity of LPS was measured by *Limulus* amoebocyte lysate (LAL) assay using the Limulus F Single Test kit (Wako, Tokyo, Japan). After purification using the Endo-free plasmid Giga kit, 1 μg/ml pDNA contained 0·01–0·05 EU/ml endotoxin. After Triton-X-114 extraction, the endotoxin levels of the DNA samples could no longer be determined by LAL assay, i.e. 1 μg/ml DNA contained less than 0·001 EU/ml. Without extraction of endotoxin by Triton-X-114, 100 μg/ml naked pDNA, which contains 1–5 EU/ml endotoxin, could release 521 ± 73 pg/ml TNF-α at 24 hr from peritoneal macrophages.

*Cationic liposome formation*

Lipofectin complexes were prepared according to the manufacturer's instructions. In brief, DNA was diluted in 100 μl Opti-MEM per 1 μg DNA (solution A) and 5 μl Lipofectin reagent was diluted in another 100 μl Opti-MEM (solution B). Then solutions A and B were combined and mixed gently. After a 15 min incubation at room temperature, complex was added to the cells.

*Cellular association experiments*

DC2.4 cells cultured in 24-well plates were washed three times with 0·5 ml Hanks' balanced salt solution (HBSS) without phenol red and 0·5 ml HBSS containing 0·1 μg/ml naked [$^{32}$P]pDNA or 0·1 μg/ml [$^{32}$P]pDNA/Lipofectin complex was added. After incubation at 37 or 4° for a specified time, the HBSS was removed and the cells were washed five times with ice-cold HBSS and then solubilized with 1·0 ml 0·3 N NaOH with 0·1% Triton-X-100. Aliquots of the cell lysate were taken for the determination of $^{32}$P radioactivity using an LSA-500 scintillation counter (Beckman, Tokyo, Japan) and the protein content was measured using the modified Lowry method with BSA as a standard.

*Confocal microscopy*

DC2.4 cells were washed three times with 1·0 ml HBSS and incubated with HBSS containing fluorescein-labelled pDNA (FL-pDNA) or FL-pDNA/Lipofectin complex. After a 3 hr incubation, the cells were washed five times and fixed with 4% paraformaldehyde for 10 min.

*Cytokine secretion*

BMDC or DC2.4 cells cultured in 24-well plates were washed three times with 0·5 ml RPMI-1640 before use. Naked DNA was diluted in 0·5 ml Opti-MEM. The cells were incubated with the naked DNA solution continuously for 8 hr. In the case of DNA/Lipofectin complexes, cells were incubated for 2 hr with 0·5 ml of the solutions containing the complexes. Then, the cells were washed with RPMI-1640 and incubated with RPMI-1640 with 10% FBS. After a 6 hr incubation, the supernatant was collected for ELISA and kept at −80°. The levels of TNF-α, IL-6, and IL-12p70 in the supernatants were determined by the OptEIA Set (BD Biosciences, San Diego, CA).

## Results

### Uptake of DNA with cationic lipid complexes is not saturated, although normal uptake is saturated in GM-CSF DC

TLR9 exists in the endosomal-lysosomal compartment.[13,14] The amount of naked DNA in the compartment can be limited because naked DNA is supposed to be taken up by DC via receptor-mediated endocytosis.[15] However, DNA/cationic lipid complexes are supposed to be taken up by DC via a non-specific mechanism based on electrostatic interaction, so-called adsorptive endocytosis. Therefore, cationic lipid Lipofectin was used to deliver DNA efficiently to the compartment. To examine the binding and uptake of naked pDNA and pDNA/cationic lipid complexes in DC, we carried out cellular uptake experiments using naked [$^{32}$P]pDNA and [$^{32}$P]pDNA/Lipofectin complexes. As expected, the uptake of naked [$^{32}$P]pDNA by DC2.4 cells at 37° was increased up to 2 hr (Fig. 1a). Following an incubation of 2–5 hr, the amount of DNA remained unchanged, probably due to continued uptake and degradation.[15] On the other hand, complexation with cationic lipids enhanced the DNA uptake. Cationic lipids enhanced [$^{32}$P]pDNA binding and